Investigation of Stage-Specific Distinction in the *Leishmania mexicana* Translational Machinery

Jiaxin Zhuo

MSc By Research

University of York

Biology

December 2024

Abstract

Leishmaniasis is a parasitic infection found in tropical, subtropical and southern European regions. The *Leishmania* life cycle is digenic and transitions between the sandfly and human hosts, which have distinct environmental conditions. Near-constitutive transcription in kinetoplasts renders gene regulation overwhelmingly post-transcriptional, placing heightened regulatory emphasis on RNA binding protein function. Modulation of translation plays a major role in parasite survival and adaptation. Our knowledge of the molecular mechanisms of translation in *Leishmania* remains limited, and it is unknown to what extent the composition of the translational machinery varies throughout the parasite life cycle Therefore, to expand this knowledge, enrichment strategies for *Leishmania* ribosomes were evaluated in order to generate samples suitable for mass spectrometry analysis of stage-specific ribosome-associated proteins. Immunoprecipitation was employed using antibodies against ribosomal protein P0 (also known as uL10) to capture the ribosomes on beads, which were subsequently analysed by mass spectrometry. Polysome profiling was also performed to identify the ideal conditions for RNA digestion to ensure the enrichment of ribosomes, to isolate both translating and non-translating ribosomes from *L. mexicana* promastigote stages and specifically exclude any RNA binding proteins (RBPs) interacting with an mRNA mid-translation. Further optimisation is required to realise this strategy. Bioinformatic analyses of mass spectrometry data have enabled comparisons of the translational machinery between the procyclic (PCF) and the metacyclic promastigotes (META). This has highlighted differentially abundant proteins involved in specific processes, which are key to cell regulation, translation and differentiation. It also illustrates how post-translational modifications (PTM) promote parasitic adaptation; specifically, protein kinase activity and phosphoregulation in META differentiation and metacyclogenesis. Key findings from our mass spectrometry include the enrichment of CRK9, RDK2 kinases and serine/threonine phosphatases in META.

Author's Declaration

I declare that this thesis is a presentation of original work and I am the sole author. This work has not previously been presented for a degree or other qualification at this University or elsewhere. All sources are acknowledged as references.

Acknowledgements

I would like to extend my gratitude to supervisors Dr Pegine Walrad and Dr Chris Hill for their mentorship and support throughout my Master's by Research. I would also like to thank them both for giving me the opportunity to work on an interesting project that uses interdisciplinary fields. I would also like to thank my Thesis Advisory Panel member, Dr Michael Plevin for his support and useful advice.

I would like to thank Dr Natalia Teles for her support, training, and willingness to help. Her guidance has made me a more confident person. I would also like to thank the other members of the Walrad lab, Hill lab, Kaye lab, Mottram lab, and the data science team for always being happy to answer any questions and making me feel comfortable and welcomed.

Table of Contents

1. Introduction

1.1 Leishmaniasis - The Disease

Leishmaniasis is a vector-borne disease caused by protozoan Kinetoplastid parasites, from over 20 different *Leishmania* species. These parasites are transmitted to humans by the bite of an infected phlebotomine sandfly, of the *Diptera* family, *Psychodidae* genera, subdivided into *Phlebotomus,* found in Asia, the Middle East, Africa and Southern European and *Lutzomyia* found exclusively in North and South America [1]. Leishmaniasis is the 9th largest global infectious disease burden and is among the top 10 most neglected tropical diseases, causing approximately 0.7 - 1 million cases per annum, with 350 million people at risk of infection [2].

There are three main forms of Leishmaniasis: Visceral leishmaniasis (VL) also known as kala-azar, cutaneous leishmaniasis (CL) and mucocutaneous leishmaniasis (ML). VL is fatal if left untreated in over 95% of cases. It is characterised by irregular bouts of fever, weight loss, enlargement of the spleen and liver, and anaemia. Most cases occur in Brazil, east Africa and India. An estimated 50,000 to 90,000 new cases of VL occur worldwide annually. It has an outbreak and mortality potential [3]. ML leads to partial or complete destruction of mucous membranes of the nose, mouth and throat [4]. CL infections in humans are caused by several *Leishmania* species including *L. mexicana* and *L. major,* and are characterised by self-healing skin lesions. This form of Leishmaniasis accounts for about 75% of infections. [3], [5]. Poor sanitation and infrequent waste removal can become a breeding site for these sandflies, which will inevitably increase the risk of infection [6]. The disease affects some of the world's poorest people as it is associated with malnutrition, population displacement, and weak immune systems.

Additionally, poor living conditions, poor hygiene and limited access to early treatment increase the chance of severity of the disease, and ultimately, transmission of the parasite. In disease-endemic countries, preventive measures are limited and safe and effective treatments are often unavailable. Existing treatments have varying efficacy, serious toxicities and substantial side effects; only one is suitable for oral administration, and the rest are

administered intravenously or intramuscularly. Therefore, there is an urgent need to find a new, effective, safe, and accessible treatment for patients [7].

1.2 *Leishmania* - The Parasite and the Cell Biology

Leishmania. spp are flagellated unicellular, digenetic parasites and have a eukaryotic cellular organisation. The shape and structure of the parasite are intricately related to their pathogenicity and their virulence. The parasite has a complex life cycle, characterised by multiple promastigotes and one amastigote (AMA) form (Figure 1) [8]. During the promastigote stages, including both procyclic (PCF) and metacyclic (META) promastigotes, the body of the parasite is an elongated spindle with a singular flagellum. The PCF promastigotes are highly polarised cells that possess several single-copy organelles with defined subcellular locations. The generation of viable progeny is heavily dependent on the precise control of the replication and segregation of organelles in the parasite [9]. The META promastigotes have the same elongated shape as the PCF promastigotes, however, they are slightly shorter body, but have a longer flagellum, as this stage is the most motile stage and requires a lot of swimming. The AMA stage takes upon a reduced form, it becomes a more spherical shape and has a short immotile flagellum which protrudes from the flagellar pocket. Some studies suggest that this flagellum is used for sensory functions [10]. This dramatic change in the cell shape results in the minimisation of the cell surface-to-volume ratio and therefore reduces the area over which the cell is exposed to the harsh environment. Both forms of the parasite contain a nucleus and a single large DNA-containing mitochondria (kinetoplast), which is one of the factors that make kinetoplasts different from classic eukaryotes.

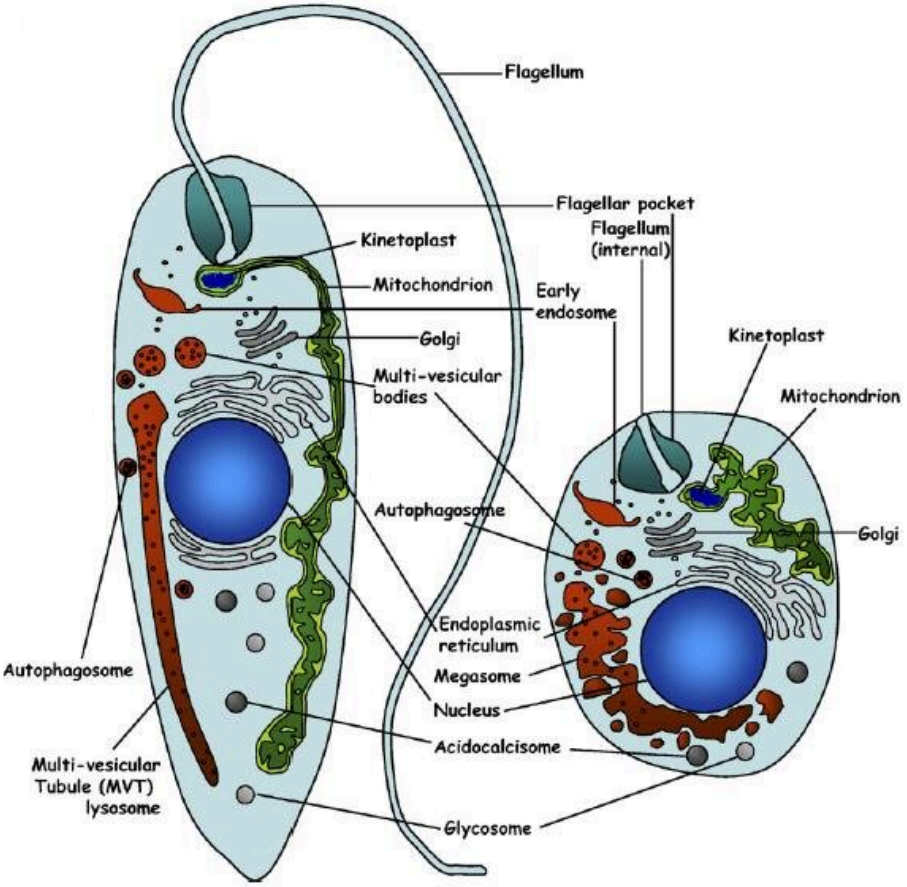

Figure 1: The structure of a *Leishmania* parasite, with both morphologies. Promastigotes on the left, with an elongated shape and amastigotes on the right, with a more spherical shape [8].

1.3 The Life Cycle of *Leishmania*

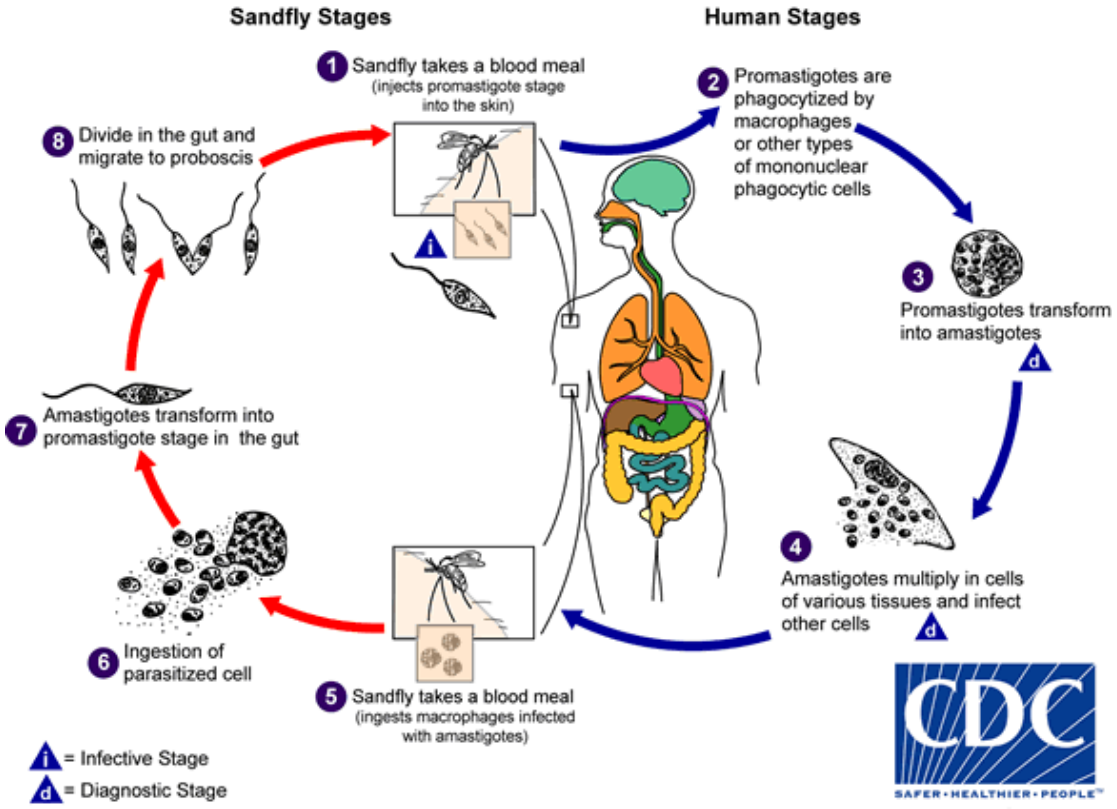

Figure 2: The *Leishmania* life cycle. This image was taken from the cdc.gov website. This depicts the life cycle of Leishmaniasis, and how it can move from one host to another. Starting in the sandfly and then being transmitted to humans, it cycles back with different forms in each stage of its life cycle.

The *Leishmania* parasites are digenic and have evolved to differentiate and multiply in two vastly different host environments. Promastigotes undergo various morphological forms within the sandfly, starting with the procyclic form, which is highly replicative in the abdominal gut then progressing into the highly mobile and infectious metacyclic form. The metacyclic form is characterised by a substantial decrease in every type of RNA, protein and lipid turnover [11]. Nutritional stress promotes the differentiation of virulent META, rendering them quiescent as they have a reduced translation rate and have the appearance of stress granules that store stalled ribosomes [12]. The META is in the lumen of the anterior midgut and foregut, ready for transmission to the mammalian host during a subsequent blood meal [13], [14]. Upon transmission of the META promastigotes to the mammalian host, the promastigotes are rapidly phagocytosed by tissue macrophages and, initially, are

contained within the phagosomes that later develop into the phagolysosomes (Figure 2). The promastigotes then differentiate into amastigotes and proliferate within the acidic phagolysosome compartment. The AMA life stage within the mammalian host may be persistent for several months or years, resulting in disease. These environments in the hosts would normally digest, degrade or destroy foreign pathogens, yet these parasites have been able to adapt and have developed resistant mechanisms to evade digestion enzymes in the sandfly and innate immune responses in mammalian animals [15], [16]. The parasite requires precise coordination of gene regulation to survive distinct environments, through changes in temperature and pH between the different hosts. This is achieved through a series of morphological, metabolic and proteomic changes carefully regulated by gene expression, which is heavily dependent on the translational machinery of the parasite.

1.4 Translational Machinery

Ribosomes are translational machinery that are among the largest and most dynamic molecular machinery. Ribosomes are crucial for protein synthesis, predominantly for the process of translation, which are finely coordinated to enable cell growth, proliferation and differentiation. Eukaryotic ribosomes are 80S ribosomes (Figure 3) made up of a large subunit (60S) that contains the 28S, 5.8S, and 5S rRNAs and roughly 45 proteins, and a small subunit (40S) that is made up of an 18S rRNA and about 30 proteins [17]. Ribosomes have universally conserved core compositions, but outside the core ribosome composition, there is great variability in ribosome-associated proteins [18], which is the subject of this thesis, specifically in the species, *L. mexicana*. Ribosome variability in *Leishmania* is of particular interest due to the parasite's life cycle stages and how the parasite can be highly replicative in one life cycle stage and be quiescent in the sequential life cycle stage. Quiescence is a reversible cellular transitory growth pause when they enter a state of dormancy during replication, but they retain the capacity to revert back to a proliferative state. This drastic change is of interest to understanding the parasite, figuring out what mechanisms and molecules are involved, in addition, how they can survive and evade such extreme and drastic environments. This is essential as it enables organisms to respond effectively to stressors or changes in nutrient availability [19]. Understanding how ribosomal proteins

contribute to these transitions may offer new insights into the parasite's survival mechanisms.

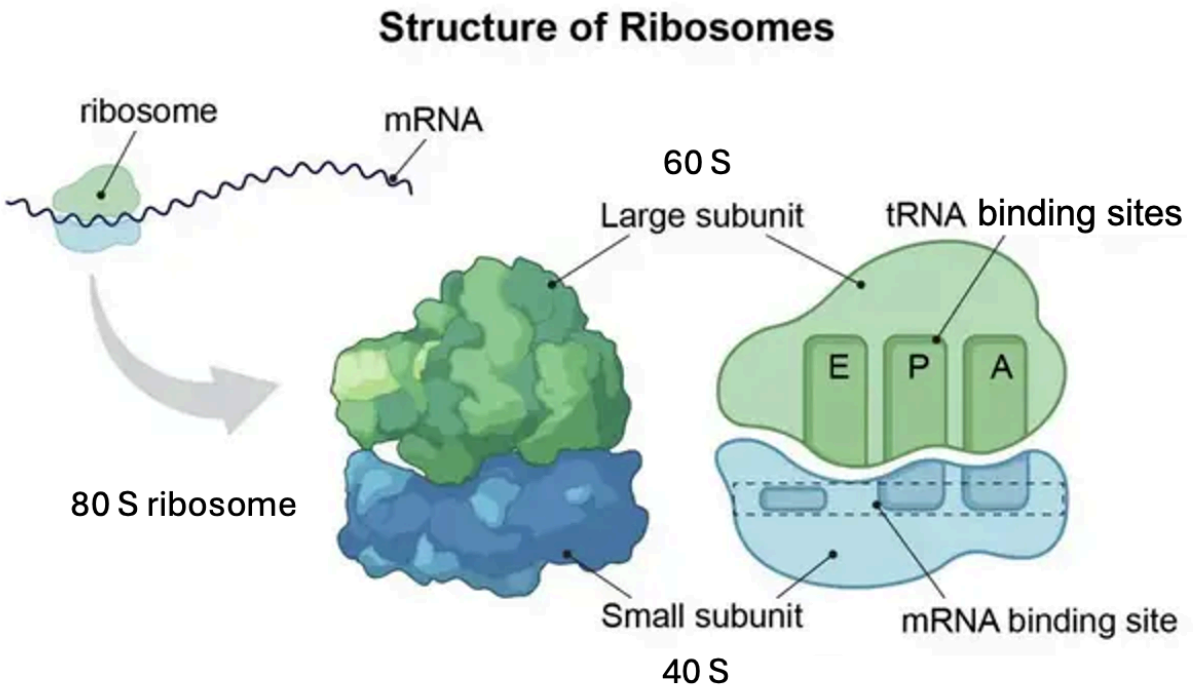

Figure 3: Overview of the 80S ribosome structure, consisting of the 60S (green) and 40S (blue) subunits, with their tRNA binding sites: A, P, E - aminoacyl, peptidyl and exit. Images created using Biorender.com

1.5 Translation in Eukaryotes

Translation, also known as protein synthesis, is a fundamental biological process in which the genetic code contained in messenger RNA (mRNA) is decoded to direct the polymerisation of amino acids. In eukaryotes, translation is highly regulated and is mediated by the ribosome. The complex interplay of ribosomal subunits, initiation and elongation factors, and mRNA ensures that translation proceeds accurately and efficiently. From the formation of the pre-initiation complex to the precise addition of amino acids during elongation and eventual termination, each step is meticulously regulated to ensure gene expression integrity at the protein level. Translation occurs in three stages: initiation, elongation and termination. Initiation starts with the 40S subunit. The ribosome consists of three tRNA binding sites (Figure 3): the A site where incoming aminoacyl tRNA enters carrying specific amino acids corresponding to the mRNA codon (and rejects non-cognate tRNAs), the P site

where peptide bonds form between amino acids and the E site where the tRNA exits after delivering the amino acid [20]. These sites are important for protein synthesis.

The process of translation begins with the assembly of the translation machinery which requires several initiation factors eIF1, eIF1A and eIF3 that bind to the 40S ribosomal subunit, these factors prime the ribosome for translation. A critical step of the initiation involves the attachment of the charged initiator tRNA (Met-tRNAi^{met}) which binds to the small ribosomal subunit at the P site [95]. This binding is mediated by the initiation factor eIF2 which is bound to a guanosine triphosphate (GTP) [21]. Together, this comprises the 43S pre-initiation complex. This complex is further stabilised by eIF5B which is also GTP-bound. The mRNA that is ready to be translated is often modified for efficient recognition by the ribosome. The mRNA molecules have a 7-methylguanosine (m7G) cap at the 5′ end and a poly(A) tail at the 3′ end. The eIF4F complex, (comprising eIF4E, eIF4A and the scaffold eIF4G) interacts directly with the mRNA. eIF4E binds to the m7G cap and eIF4G, whilst poly(A) binding protein (PABP) binds to both the poly(A) tail and eIF4G, thus circularising the mRNA. eIF4A is an ATP-dependent RNA helicase, which aids the ribosome in resolving secondary structures in the mRNA [95]. The 43S pre-initiation complex binds to the mRNA, forming the 48S complex. This complex moves along the mRNA chain toward its 3'-end, in a process known as 'scanning', to search for the AUG start codon [100]. Upon recognition of the start codon, GTP is hydrolysed and the initiation factors bound to the 40S subunit dissociate. The 60S ribosomal subunit is then recruited for the 80S ribosome complex, once this is formed elongation can begin [96], [97].

Elongation is the stepwise addition of amino acids to the growing polypeptide chain, driven by the elongation factor GTPases eEF1a and eEF2. eEF1a delivers the charged aminoacyl-tRNA to the A site of the ribosome [95]. The anticodon of the tRNA must match the mRNA codon in the A site, ensuring the correct amino acid is incorporated into the polypeptide chain. Once the correct tRNA is in place, eEF1a hydrolyses GTP, releasing the tRNA for accommodation into the peptidyl transferase centre in the 60S subunit, and the ribosome catalyses the formation of a peptide bond between the peptidyl-tRNA in the P site and the aminoacyl-tRNA in the A site [95], [98]. As a result, the growing peptide chain is transferred to the tRNA in the A site. Following this, the ribosome spontaneously adopts a

rotated state, and reverse rotation is facilitated by eEF2 binding and GTP hydrolysis, allowing it to translocate along the mRNA by one codon. This shifts the now-deacylated tRNA to the E site, where it exits the ribosome, and the tRNA holding the growing polypeptide moves to the P site. A new charged tRNA enters the A site, and the cycle continues [96], [97], [98].

Termination occurs when the ribosome encounters a stop codon (UAA, UAG, or UGA) in the A site. These codons do not correspond to any tRNA; instead, they are recognised by a protein release factor called eRF1 [98], [99]. eRF1 binds to the ribosome and catalyses the cleavage of the bond between the polypeptide chain and the tRNA in the P site, releasing the newly synthesised protein [99]. Once the polypeptide is released, the ribosome dissociates into its 40S and 60S subunits, completing the translation process.

1.6 Translation in Kinetoplastids

Trypanosomes (*Trypanosoma cruzi* and *Trypanosoma brucei)* and *Leishmania* are both kinetoplastid parasites that share unique ribosomal features. Kinetoplastid ribosomes consist of six fragments of the large subunit rRNA unlike the single 28S rRNA found in most eukaryotes [39]. The structure of the ribosomes can significantly vary between species. Notably, in kinetoplasts, the rRNA expansion segments are enlarged compared to other eukaryotes. The enlarged expansions and ribosomal-protein extensions lead to the formation of additional inter-subunit bridges, not present in other eukaryotes [83], [84]. These expansion segments are thought to play a major role in ribosome function and stability. Such differences could highlight the evolutionary adaptations of the ribosome in various organisms [39], [84].

They also share unique post-transcriptional gene regulatory mechanisms critical for survival across diverse environments. Trypanosomes differ from other eukaryotes due to the control gene expression via transcriptional regulation, as they rely on polycistronic transcription, resulting in polycistronic mRNAs processed into monocistronic mRNAs by trans-splicing and polyadenylation [25], [26]. This process requires translation efficiency and mRNA stability to maintain gene expression regulation [22]. Factors that are key to gene regulation are

RNA-binding proteins that target the 3’- untranslated regions (UTR) of mRNAs, enhancing or reducing stability and translation. Trypanosomes exhibit six homologues of cap-binding initiation factors, a novel decapping enzyme, and an mRNA-stabilising complex that enhances adaptability in changing host environments [23]. *Trypanosoma brucei* has been studied more extensively, and insights from these studies provide a valuable framework and foundation for understanding similar mechanisms in *Leishmania*.

In *Leishmania*, translational control is pivotal for adapting to rapid environmental shifts between hosts. Studies show that *Leishmania* relies on translational regulation through RNA-binding proteins to modulate gene expression at the mRNA level [24]. This parasite also undergoes polycistronic transcription. Unlike most eukaryotes, *Leishmania* lacks traditional transcriptional control, making post-transcriptional and translational regulation crucial. Regulatory elements in the 3'-UTR drive this process, which is key to conserving energy and adapting protein synthesis for survival across environments [27]. These mechanisms allow *Leishmania* to adapt across life stages, though specific ribosomal regulation throughout its lifecycle is still largely unexplored.

Together, these mechanisms highlight how kinetoplastid parasites like trypanosomes and *Leishmania* rely on specialised translational and post-transcriptional regulation to thrive under varied and often hostile conditions. It is poorly understood what molecular components are involved in the regulation of translation during environmental stresses and changes of hosts and the changes through the different life cycles. Also, the role of RNA-binding proteins and 3’ UTRs in mRNA stability and translation is not fully characterised, leaving gaps in understanding how these elements function in *Leishmania* [12]. The lack of transcriptional regulation means that the parasite is heavily reliant on post-transcription processes which complicates the understanding of its translational control. The parasite’s adaptation to environmental changes, such as temperature and pH, involves translational control, but the precise molecular pathway remains unclear [28]. A better understanding of the ribosome will help us to understand how the parasite adapts to its host environment and how it evades the immune system and transitions between the life cycle stages, each of which has different metabolic needs. The identification of *Leishmania*-specific

ribosome-associated proteins will also allow us to determine how *Leishmania* and *Trypanosoma* vary in translation and gene regulation.

1.7. Specialised Ribosomes and Hibernation Factors

Recent studies have indicated that ribosomes are not uniform, they exhibit significant heterogeneity and specialisation based on environmental conditions and cellular contexts [29], [30], [31]. Other studies have shown that heterogeneous ribosomes display functional specialisations that can boost the translation of selective sub-pools of mRNA [32] and it has been demonstrated that ribosomes expressing heterogeneities might be a stress response [33]. *Leishmania* undergoes a lot of environmental stress; they alternate between different hosts and the environments change drastically between them. This challenges the traditional view of ribosomes as identical entities, suggesting a more complex regulatory framework for protein synthesis [34].

There have also been studies focused on hibernation factors. Hibernation factors are proteins that inhibit protein synthesis to protect the ribosomes from degradation, especially when organisms encounter unfavourable conditions [35]. This is done to ensure the overall reduction of protein synthesis which is metabolically expensive while maintaining a basal level of translation. Hibernation factors seem to be predominantly produced in the stationary phase in bacteria during its growth cycle [36]. If a hibernation factor were to be discovered, it would be expected to be in the META stage of the life cycle. During the META stage, the parasite enters the stationary phase, where replication is depleted and so there are reduced levels of translational levels. Identifying ribosome specialisation or any hibernation factors would be of great interest to the field and would aid in understanding the parasite's molecular capacity to survive its hosts. A hallmark of *Leishmania* is that it can adapt to unpredictable fluctuations inside the human host, which is why it has been proven difficult to find a treatment against this parasite.

1.8 Purpose, Aims and Strategies

This project draws upon the de Pablos *et al.,* 2019 [43] study of the RNA-binding proteome (RBPome) of *L. mexicana* between the different lifecycle stages, which quantitatively defines and compares the mRBPome of multiple stages in kinetoplastid parasites, and provides insights into the trans-regulatory mRNA:protein complexes that drive *Leishmania* parasite life cycle progression. The study highlighted the importance of gene regulation across the three main lifecycle stages of *Leishmania*. It also indicated stage-specific heterogeneity in protein expression relative to RNA binding capacity, demonstrating the parasite's life cycle stages significantly affect its molecular behaviour. Therefore, we aim to isolate ribosomes from different stages of the *L. mexicana spp* parasite to identify any compositional variation or differences in ribosome-associated factors that may be involved in the regulation of translation. Our main focus will be the procyclic and metacyclic promastigotes as they are both part of the promastigotes stage but have highly diverse characteristics. The assessment of any life cycle-specific molecular components will assist in explaining how the parasite can alternate between highly replicative and quiescent states as they occur sequentially in the life cycle. Furthermore, any parasite-specific ribosomal attributes may be relevant in discovering combative strategies.

This project focuses on developing strategies for isolating ribosomes in order to detect stage-specific variations in ribosomal proteins or ribosome-associated factors by mass spectrometry. Here I intend to outline the cell fractionation experiments and demonstrate ribosome enrichment through immunoprecipitations. However, in translationally-active cells, ribosomes will form polysomes on mRNA molecules, and immunoprecipitation of polysomes will also enrich mRNA-bound proteins. Therefore, I also present polysome profiling experiments to determine the optimum RNAse digestion strategy to isolate monosomes for mass spectrometry. This requires further optimisation.

Overall, this approach will allow me to compare ribosome-associated proteins between key lifecycle stages and explore potential ribosomal modifications linked to the life cycle transitions. In future, compositional variations of *Leishmania* ribosomes will be further investigated by cryo-EM. Identifying the molecular components of the translational

machinery that allow the parasite to proliferate and grow in distinct hosts may ultimately enable the identification of potential pharmacological targets as well as the development of novel treatments and therapies.

2. Materials and Methods

2.1 Parasite Cell Culture and Purification

Procyclic promastigotes forms (PCF) of WT *L. mexicana* (strain M379) were grown in M199 medium (5x M199 (Gibco #10012037), 10% heat-inactivated foetal bovine serum (hiFBS), 1M HEPES-NaOH, pH 7.4, 5.0 mM adenine, with an antibiotic of 1% penicillin/streptomycin and 0.25% Hemin) at 1 x 10^5 cells/ml at Day 0 and were cultured at 26 °C for three and a half days (Figure 7), these were to isolate the parasite in log phase (3-6 x10^6 cells/ml). These cells were treated with 100 µg/ml of cycloheximide (CHX) and incubated for 10 min at 26 °C. The parasites were then centrifuged at 800 x g at 4 °C and washed twice with 1 x PBS supplemented with 100 µg/ml of CHX and snap-frozen in liquid nitrogen for storage.

To isolate the metacyclic promastigotes forms (META), the PCF forms were inoculated from the M199 media into Grace's Insect Culture media (Grace's' media powder (Sigma G9771) supplemented with 10 % hiFBS, 1% penicillin/streptomycin, 1X Basal Medium Eagle (BME) vitamins at pH 5.5) at a cell density of 1.5x 10^5 cells/ml and were cultured for seven days at 26 °C. This allows synchronous population transformation of the parasite from the procyclic to the metacyclic life cycle stage. The parasites were isolated in stationary phases (2-4 x10^7 cells/mL). Prior to harvest, parasites were treated with 100 µg/ml CHX and incubated for 10 min at 26 °C, washed twice with 1 x PBS (137 mM NaCl, 2.7 mM KCl, 10 mM Na_2HPO_4, and 1.8 mM KH_2PO_4) supplemented with 100 µg/ml CHX, before snap-freezing in liquid nitrogen for storage.

2.2 Immunoprecipitation

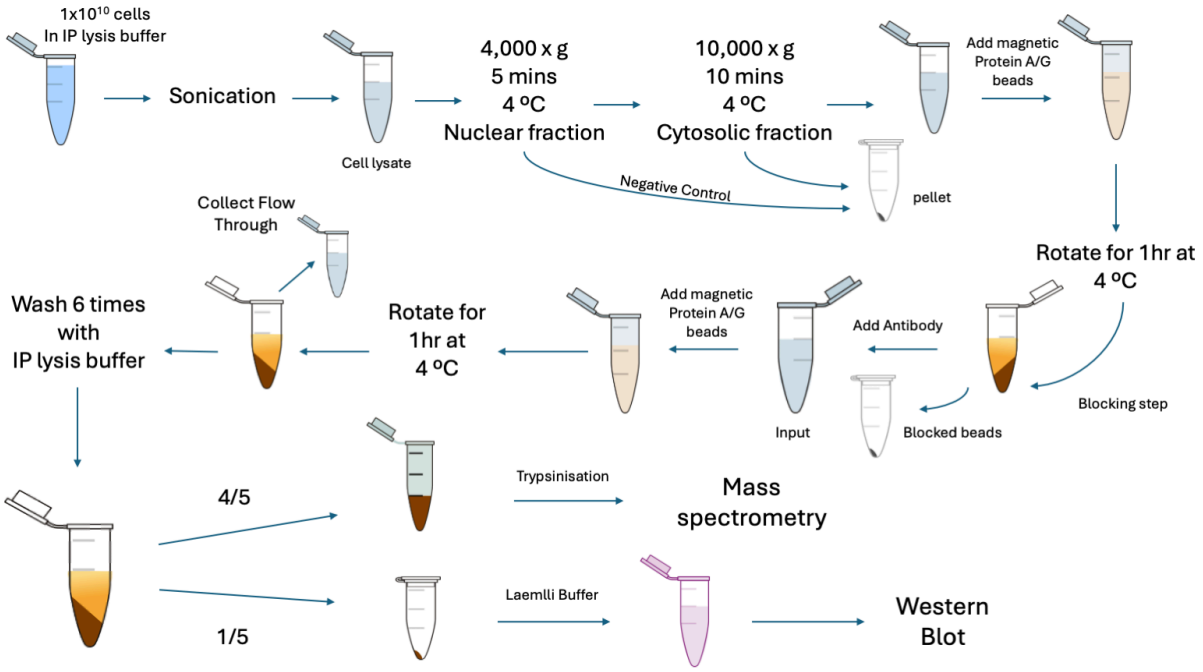

Figure 4: Overview of the immunoprecipitation experiment. Highlighting the blocking step, the block beads are the background protein. Each sample was given 2mg / 100 µl of Protein A/G beads at both stages. TcP0 was the antibody used and 1:1000 of the antibody was used. After each wash, the supernatant was collected. Once the washing step was completed the beads were split and sent for analysis.

PCF and META samples were used for this experiment. A total of ~1 x 10^{10} cells, resuspended in IP-lysis buffer (10 mM Tris HCl pH 8.0, 5 mM $MgCl_2$, 100 mM KCl, 100 µg/ml cycloheximide (CHX), 1.0 mM DTT, 1 tablet Roche cOmplete EDTA-free Protease inhibitor cocktail/15ml) and the cells were lysed via water bath sonication. This method is a gentler type of sonication which completely lyses the cells but also ensures the nuclei stay intact. After sonication, the cells were spun (4000 x g, 5 min 4 °C). The pellet from this centrifugation is the nuclear fraction. The nuclear fraction is kept as a negative control sample for the western blot. The supernatant was spun again (10 000 x g, 10 min, 4 °C) to yield the cytosolic fraction. The supernatant taken after all the debris has been removed is the input. Limited RNAse digestion was initiated by adding 250 µg/ml of RNAse A for 30 min at 25 °C, before quenching with 800 U of RiboLock, the same conditions as stated in Figure 11A.

Protein A/G magnetic beads (Bimake.com; B23202) were prepared the day before, by washing three times in lysis buffer and then diluting the beads to ensure 2.0 mg beads per 100 µl sample. A blocking step was performed by adding 100 µl of 2.0 mg of Protein A/G beads with 2.5 µl of RiboLock and incubating for 1 hr, to remove non-specific proteins that bind to the beads without any antibodies present. During the experiment, we were not aware that the beads also could potentially bind to UL10. After the beads were removed, the cleared supernatant became the input for the IP. A new set of beads with RiboLock was incubated with the *T. cruzi* P0 (uL10) antibody [1:1000] for 1 hr. The antibody-bound beads were then added to the PCF and META cell lysate samples and incubated for another 1 hr at 4 °C. The beads were then washed six times using the IP-lysis buffer. After the final wash, the beads were split into ⅕ for the western blot (see section 2.3) and ⅘ of the proteins attached to the beads were sent to mass spectroscopy (see section 2.5). The proteins for western blot are extracted by heating the beads (95 °C, 10 min) in Laemmli buffer (62.5mM Tris-HCl, pH 6.8, 2% SDS, 10% Glycerol, Bromophenol blue) supplemented with 5% β-mercaptoethanol (BME). The proteins for mass spectroscopy remain on the beads until trypsin digestion.

2.3 Western Blot

The proteins extracted in the Laemmli buffer were separated by a 12 % SDS-PAGE with 1x TGS buffer (0.25 M Tris-HCl, pH 8.3, 1.92 M Glycine, 1% SDS) (100 V, 90 min). Subsequently, this is transferred to a PVDF membrane (Immobilon®) via electroblotting (20 V, 60 min). The membrane was blocked with 5% skimmed-milk solution in phosphate-buffered saline supplemented with 0.05% Tween-20 (PBST) overnight at 4 °C, this was then washed three times with PBST for 10 min. The membrane was then incubated with the primary antibody TcP0 at room temperature for 1 hr (rabbit polyclonal, 1:5000 dilution in 1% skimmed-milk in PBST) and then washed three times with PBST for 10 min. The secondary antibody was then added. Originally, anti-rabbit IgG-horseradish peroxidase (HRP) was used (1:5000 dilution in 1% skimmed-milk in PBST) with an 1 hr incubation at room temperature. However, unexpected bands were evident when using the anti-rabbit IgG HRP. We hypothesised that these originated from a denatured primary antibody from the IP since the beads were boiled in the Laemmli buffer. Therefore, this prompted a substitution of the secondary antibody for Protein G-HRP, which only binds to non-denatured antibodies. Membranes were incubated

with Protein G-HRP (1:5000 dilution in 1% skimmed-milk in PBST) for 1 hr at room temperature, and washed as above in PBST. The western blot was developed using an ECL kit (GE Healthcare) and was recorded on the ChemiDoc.

2.4 Polysome Profiling

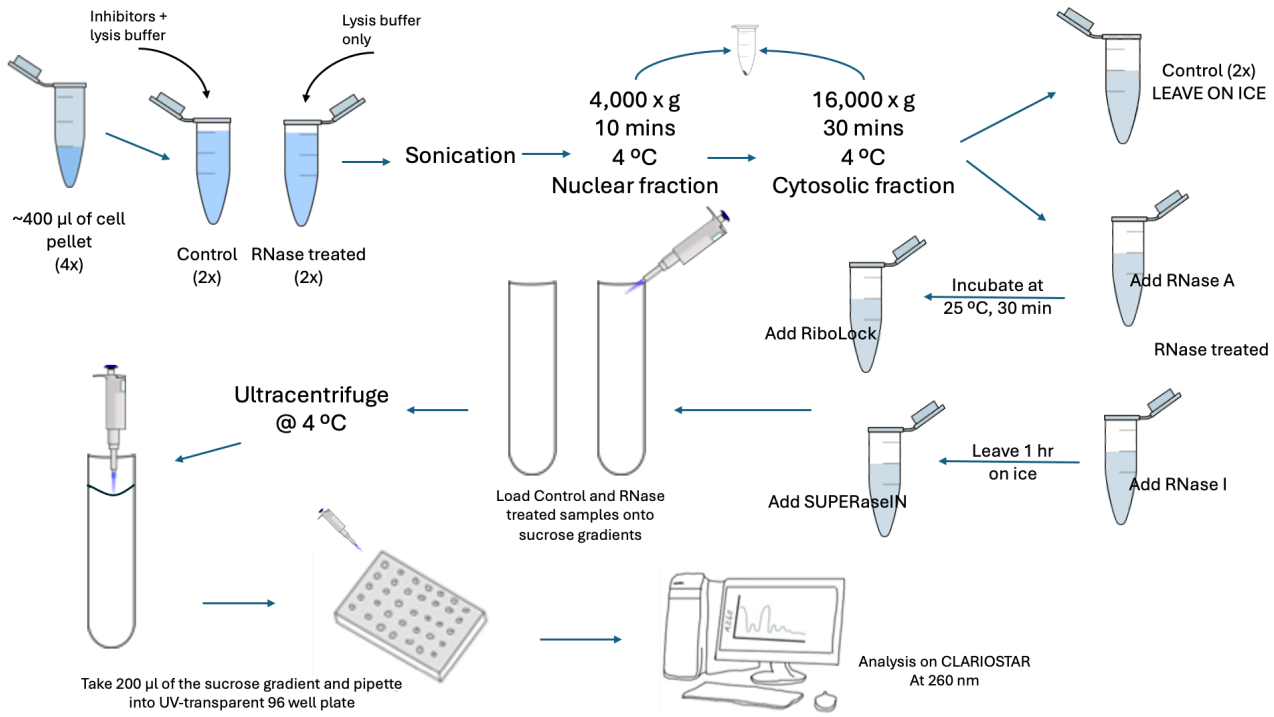

Figure 5: Overview of the polysome profiling experiment. Includes control samples, which have their respective RNA inhibitors only and the RNase-treated samples with RNase A and RNase I. The SW41 rotor is used for ultracentrifugation. Analysis on the CLARIOSTAR microplate reader (BMG Labtech) was applied using UV-transparent 96 well plates.

From the PCF harvested sample, ~2x10^9 cells were taken from frozen and thawed in 500 µl of lysis buffer (40 mM HEPES (KOH) pH7.4, 10 mM MgCl2, 100 mM KCl 250 mM, 8.5% w/v Sucrose, 0.2 mM CHX, 2.0 mM DTT, cOmplete EDTA free protease inhibitor (1 per 25 ml), DNAse I from bovine pancreas (Sigma DN25, 0.02 mg/ml). For the controls, the samples were thawed in the 500 µl of lysis buffer and in addition, an RNase inhibitor to quench any endogenous RNase already present in the sample, before sonication. This is used to compare and identify if the treated samples will make a difference. Samples were lysed via water bath

sonication at 0 °C for three minutes, and clarified by two successive centrifugation steps (first 4000 x g, 10 min, 4 °C and then 16 000 x g, 30 min, at 4 °C). The supernatant was collected and the pellets were discarded from both spins. Samples were treated with either RNase A (250 µg/ml, ThermoFisher) which was incubated at 25 °C for 30 min or RNase I (1200 U, Ambion, AM2294) followed by the addition of RiboLock (ThermoFisher) or SUPERaseIN (Ambion, AM2696) 800 U and 100 U respectively, to halt the RNase digestion. The RNase enzymes were added, and the RNase A was incubated at 25 °C for 30 min. RNase I was added and left on ice for 1 hr. After the incubation periods their respective RNase inhibitors were added RiboLock for RNase A and SUPERaseIN for RNase I and then loaded onto sucrose gradients.

RNA concentration was measured using the Nanodrop UV spectrophotometer, with an A260 = 40 per lysate sample used for each sucrose gradient. Sucrose gradients were prepared (20 mM HEPES-KOH pH 7.4, 100 mM KCl, 10 mM $MgCl_2$, 1 mM DTT, 1x cOmplete EDTA-free protease inhibitor) [12] from 10% - 50% w/v in SW41 ultracentrifuge tubes (SEATON) using a BioComp Gradient Master (BioComp Instruments) according to the manufacturer's instructions. The monosomes were purified as described in Ingolia *et al*., 2009 [90]. The control and treated samples were loaded onto the sucrose gradients and were spun at 210,000 - 254, 000 x g (31,000 - 38,000 rpm) overnight using a SW41 Ti rotor (Beckman Coulter) in an Optima TL ultracentrifuge. The gradients were manually fractionated by taking 200 µl from the meniscus and loaded into a UV-transparent 96-well plate. The CLARIOstar (BMG Labtech) was used to read the absorbance of the plates at A260.

2.5 Mass Spectrometry

Mass spectrometry analysis was performed by Adam Dowle and his team in the BTF-MAP lab. The six samples from the immunoprecipitation were on-bead digested using the Rapid immunoprecipitation mass spectrometry of endogenous proteins (RIME) protocol [57] before analysis by PASEF-DIA using an EvoSep One UPLC and Bruker timsTOF mass spectrometer [91]. Peptides were eluted from an 8 cm nano C18 column over a 100SPD elution profile with DIA (Data-independent acquisition) data acquired between *m/z* 400-1200 in 25 Th windows. Data was searched against the *L. mexicana* subset of TriTrypDB

(TriTrypDB-68_LmexicanaMHOMGT2001U1103, April 2022) using DIA-NN (1.9) setting a 1% FDR and using the high precision version of Quant-UMS with sample normalisation applied. Results were filtered to protein q<0.01 and a minimum of two peptide matches. Pair-wise group testing used limma via an in-house R-shiny installation of FragPipe-Analyst. Sample minimum imputation was applied at the point of testing and the Hochberg and Benjamini approach was used for multiple tests.

2.6 Bioinformatic Analysis

2.6.1 Protein Annotation

A list of characterised core ribosomal proteins from structural depositions to the worldwide Protein Data Bank (wwPDB) was compiled from various eukaryotic species such as yeast (4v7r, Ben-Shem *et al.*, 2010) [37], *T. bruce*i (4v8m, Hashem *et al*., 2013) [38] and *L. donovani* (5t2a, Zhang *et al*., 2016) [39]. They were annotated with the corresponding *L. mexicana* nomenclature which was found in the TriTrypDB.

2.6.2 Volcano Plots

Volcano plots were generated in RStudios using R for interactive visualization. Log2 fold change value of every protein from the mass spectrometry data was used and the adjusted *p*-value ≤ 0.05 was calculated to reveal significantly abundant proteins.

2.6.3 Venn Diagrams

Proteins of each life cycle stage were filtered into abundant PCF-specific proteins and META-specific proteins from their data-independent acquisition (DIA) intensities. Across the three replicates proteins that reached the threshold in all three replicates were considered significant to be in both life cycle stages. The proteins that had intensities in only one or two of the replicates were not considered significant to ensure reliable data. These proteins were used to create a Venn diagram in Venny (bioinfogp.cnb.csic.es/tools/venny/index.html) [40]

2.6.4 Gene Ontology Term Analysis

Gene ontology terms were found in UniProt using the ID mapping tool. Gene ontology (GO) analysis was performed to identify biological processes and molecular functions enriched in ribosomal proteins isolated from the different life cycle stages, PCF and META, relative to the predicted *L. mexicana* proteome were derived using Tritrypdb.org (04.2022) [41]. Cytoscape [81] was used to map out biological networks with the application of BiNGO [82], using the *p*-values from BiNGO this was inputted into the REVIGO software and was used to refine and visualize enriched terms (revigo.irb.hr) [42], providing insights into stage-specific translation processes.

3. Results

3.1 Visualisation of Ribosomal Proteins

Ribosomes are conserved translation machinery found in all eukaryotic cells. Before any experiments began, I sought to visualise the location of ribosomal proteins that were detected in a previous *L. mexicana* mass spectrometry dataset [43] and investigate whether the relative abundance of these proteins changed in different lifecycle stages. The structure of the *L. donovani* ribosome has been determined using cryo-EM by Zhang *et al.* 2016 (PDB ID 5T2A)[37]. This ribosome structure was used as a reference to enable the visualisation of ribosomal proteins in PyMOL. This previous study by Pablos *et al.*, 2019 [43] defined the entire mRNA-binding proteome of cross-linked cells from each lifecycle stage of *L. mexicana*. Many ribosomal proteins were present in this dataset, and I used this data to annotate the 5T2A ribosome based on relative protein abundance in comparison to the whole proteome (Figure 6).

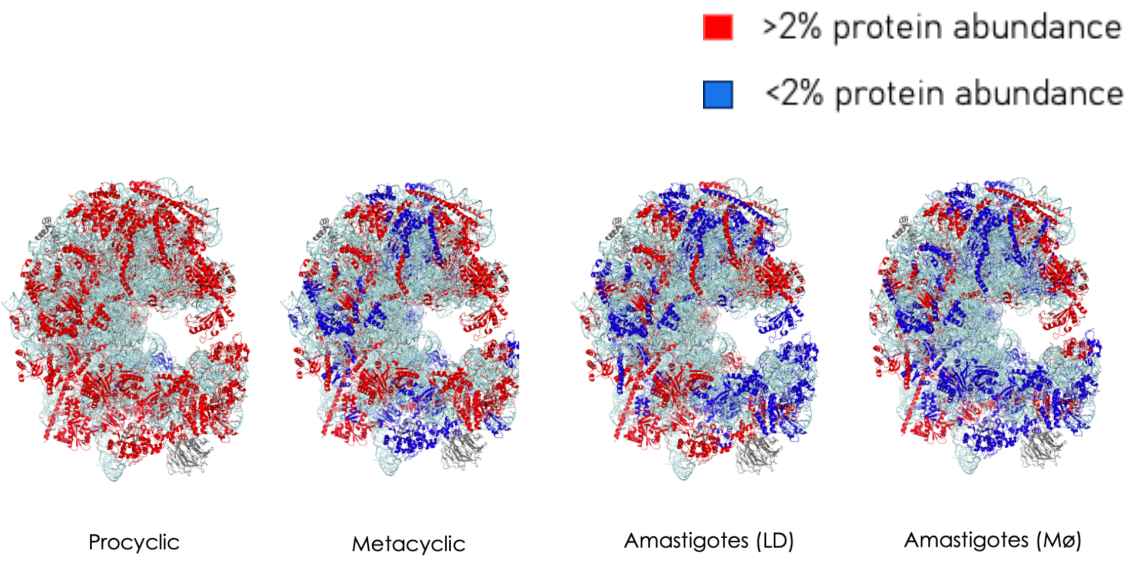

Figure 6: A schematic visualised in PyMol of crosslinked RNA-associated proteins from different life cycle stages within the *Leishmania* ribosome. The ribosome model used was 80S from *Leishmania donovani* (PDB ID: 5T2A, Zhang *et al.*, 2016) [39]. Data taken from Pablos *et al.* 2019 [43], where the mean of the triplicate repeats of protein abundance was identified of three main life cycle stages (procyclic promastigote, metacyclic promastigote, lesion-derived amastigotes (AMA LD) - and mouse macrophage-derived amastigotes (AMA Mø).

Red represents protein abundance >2% and blue indicates protein abundance <2%. Cyan represents the rRNA structure of the ribosome and grey represents the ribosomal proteins that were not detected by mass spectrometry in Pablos et al. 2019 [43].

Ribosomes core proteins are conserved between *Leishmania* species, therefore we expect to see similar protein enrichment between the *L. donovani* and *L. mexicana* translational machinery. Core ribosomal proteins were identified in the dataset from Pablos *et al.*, 2019 [43], indicating sufficient coverage of ribosomal proteins to infer differences in relative abundance between the life cycle stages. Figure 6 indicates that ribosomal proteins are most abundant in the procyclic promastigote stage and ribosomal protein enrichment decreases as the life cycle progresses, in META, AMA LD and AMA Mø lifecycle stages. This could be due to the cells becoming quiescent and less replicative in the later stages. We would expect to see a decrease in all ribosome proteins when entering quiescence. As ribosome proteins all occur in a 1:1 ratio per ribosome, we would expect to see all "blue" in later stages. However, it is observed that some proteins are still in “red”, where the protein abundance is >2 % in the later stages (Figure 6). This could be evidence of stoichiometry variation, suggesting that the composition of ribosomes can adapt to different environmental stimuli, which can influence their translational capacity [89]. Some ribosomal proteins may be in excess due to paralogues in the ribosomal genome. Paralogues can contribute to the functional diversity of ribosomes, allowing for specialised functions under varying conditions, particularly in the context of quiescence, where different ribosomal compositions may be necessary to adapt under stress [89]. This supports the hypothesis for ribosome variation in different lifecycle stages.

3.2 Parasite Growth for Optimal Harvesting

Leishmania M379 strain (wildtype) cells were diluted with filtered isotone in a 1:100 dilution. Cells were counted using the ZI Coulter Particle Counter over a period of 10 days to determine the optimal harvesting window, to isolate the parasites at the PCF and META forms. Figure 7 shows the optimal window to harvest the cells and isolate them at the specific life cycle stage. For PCF (3-6 $x10^6$), this is about 3.5 days and for META (2-4 $x10^7$), it ranges from 5 to 8.5 days. A double purification of Ficoll + human complement would

guarantee a greater quantity of META and remove any PCF that have not differentiated yet, however, the META were not purified, which could have affected results later downstream.

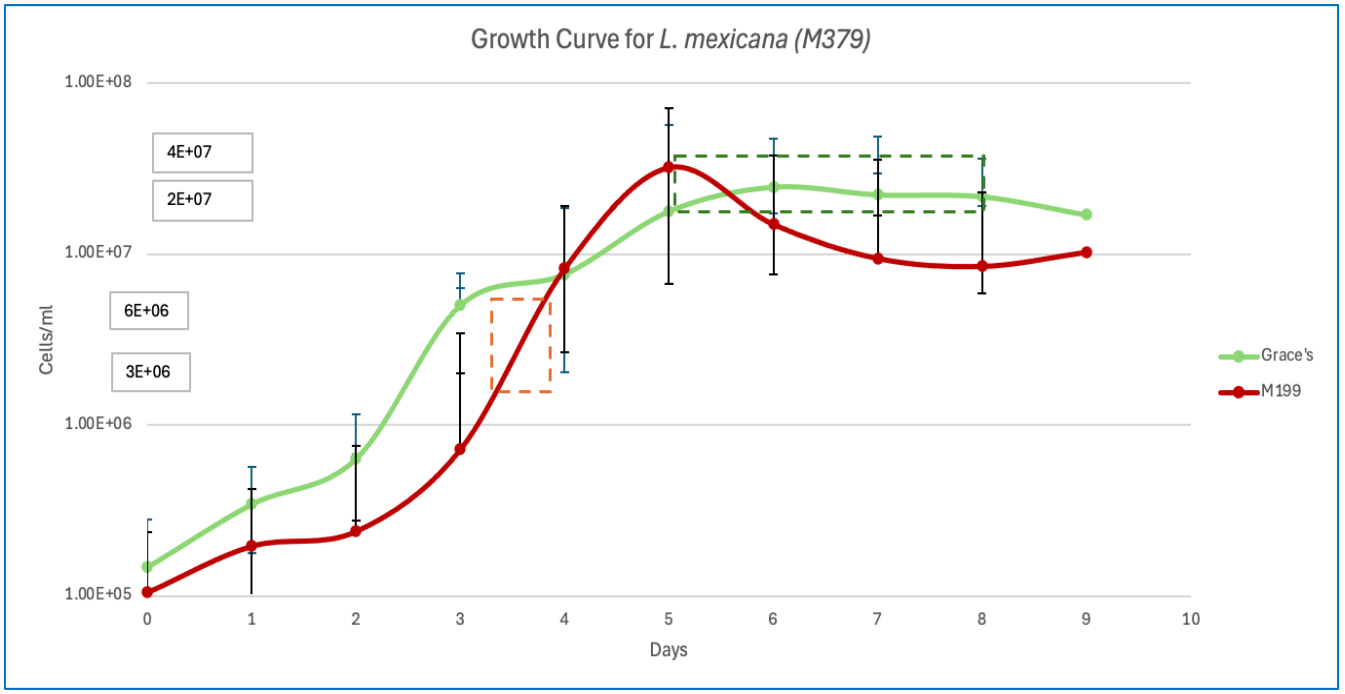

Figure 7: The growth curve represents the average growth of the WT *L. mexicana* M379 parasites in the M199 media (red) and Grace's Insect media (green). With the number of days on the x-axis and cells/ml on the y-axis. The dashed orange lines represent the optimal window in which the cells are at 3-6e+06 (3-6 $x10^6$) for the PCF harvesting. The dashed dark green lines represent the optimal window in which the cells are at 2-4e+07 (2-4 $x10^7$) for the META harvesting. SD bars were added to represent the variation between the repeats of growing these cells.

Figure 7 shows the parasites are grown in different mediums. M199 (red) promotes the initial growth of PCF promastigotes, but does not facilitate the differentiation of META promastigotes as easily, whereas Grace's Insect Medium provides a higher proportion of META compared to M199 media [44]. Therefore, M199 media was used to culture the PCF and Grace's Insect Medium to culture the META for optimum growth and differentiation.

3.3 Validation of LmXP0/LmXuL10

The P0 protein is part of the ribosomal eukaryotic stalk, an elongated lateral protuberance of the large ribosomal subunit, and is involved in the interaction of elongation factors [45]. Western blots validated the P0 (uL10) presence in *L. mexicana* using a rabbit polyclonal anti-TcP0 antibody created against *Trypanosoma cruzi.* P0 is highly conserved in other eukaryotes as the alignment of the deduced primary structure of the *T. cruzi* P0 (TcP0) compared with human P0 (HuP0), yeast P0 (YP0) and *Leishmania chagasi* P0 (LcP0) contains sections of identical sequences. TcP0 exhibits an overall homology of 58% with HuP0, 62% with YP0 and 84% with LcP0, thereby indicating a significant degree of similarity in the characteristics of these proteins [46][92]. To date, there appears to be a lack of research directly comparing the conservation of P0 protein between *T. cruzi* and *L. mexicana.* Nonetheless, it is reasonable to assume that P0 is highly conserved, as evidenced by the similarities between LcP0 and TcP0 [92], given that *Leishmania spp.* are known to be highly conserved [93]. Consequently, it is hypothesised that the TcP0 antibody would be able to pull down the ribosome in *L. mexicana*, facilitating ribosome enrichment and isolation. The molecular weight of TcP0 was estimated to be 34 kDa [47], and we observed a band corresponding to LmxP0 around 37 kDa by western blot (Figure 8).

Once the LmxuL10 (P0) expression was verified in both PCF and META cells, this antibody was used to immunoprecipitate LmxuL10 to isolate associated ribosomes in both these promastigote stages. Western blots confirm the integrity of the IPs and successful elution of LmxuL10 in triplicate in both stages (Figure 8).

PCF 1

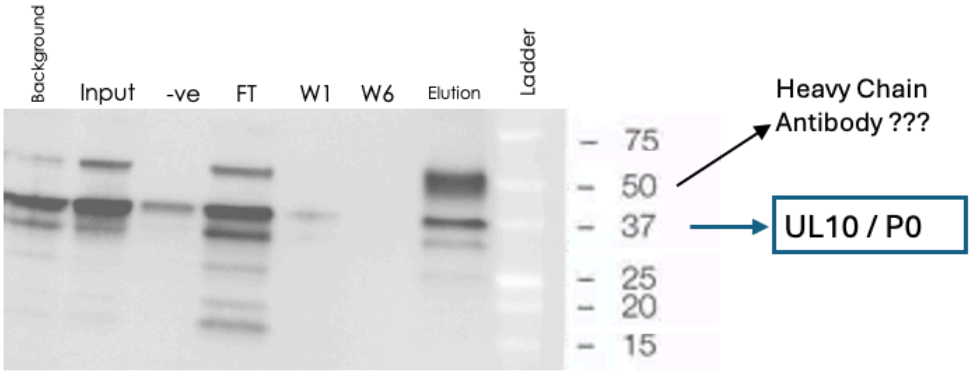

PCF 2

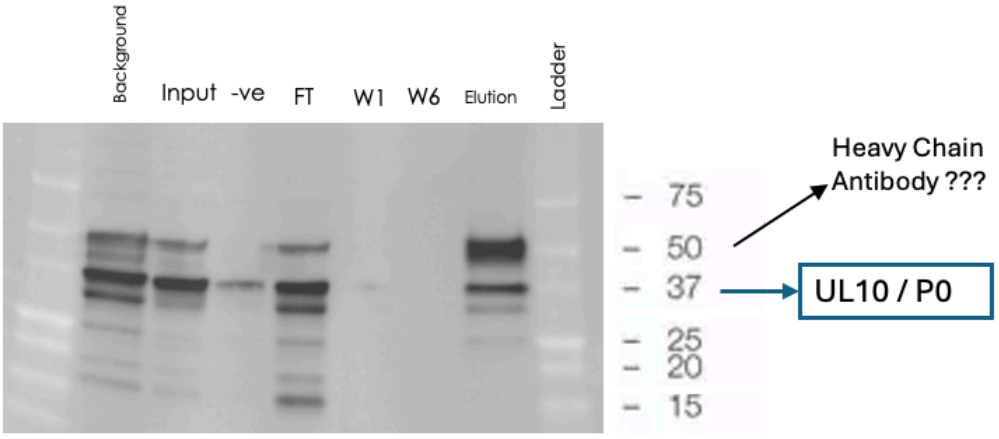

PCF 3

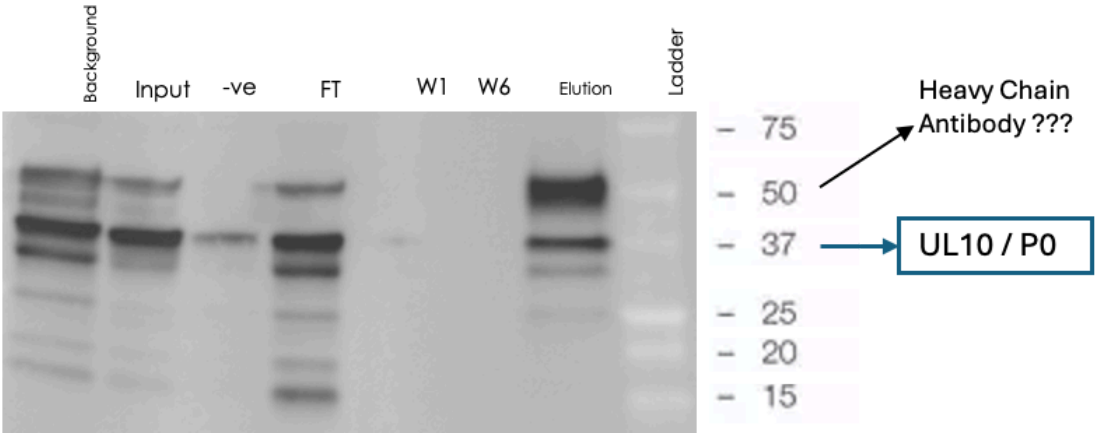

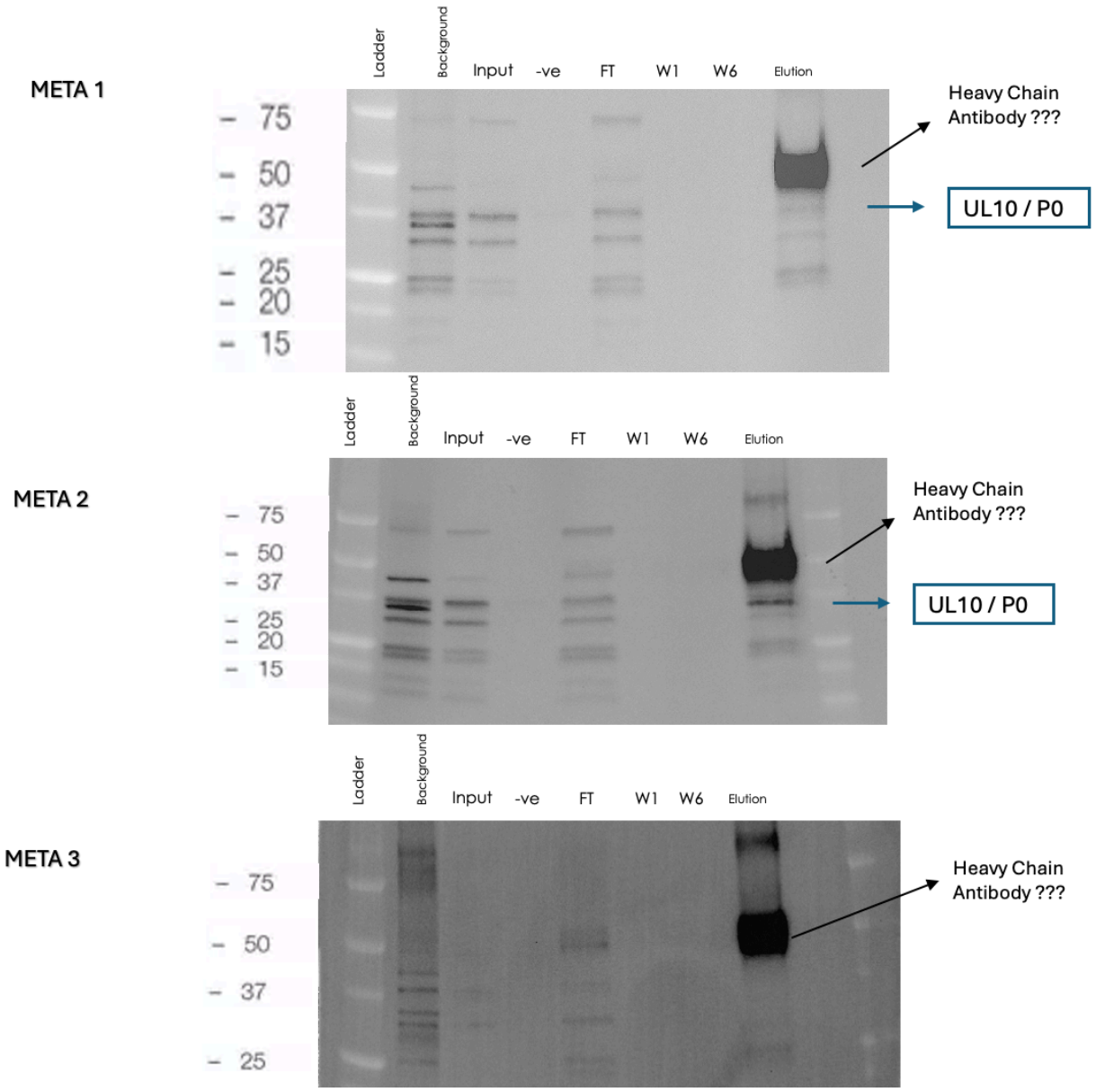

Figure 8: Western blot analyses (in triplicate) of P0 (uL10) immunoprecipitations from PCF and META cells - 3 different samples of the same lifecycle stage. In these experiments, anti-Rabbit-HRP was used as the secondary antibody. Refer to Figure 4, to understand how each well sample was obtained. For the **ladder,** we used Precision Plus Protein All Blue. The **background** is proteins that bind to the Protein A/G beads before antibody incubation, this is the blocking step. The **Input** is the cytosolic fraction. **Negative control (-ve)** is the nuclear fraction. **FT** is flow through, **W1** is the first wash, **W6** is the last wash, and **Elution** of the proteins obtained from the immunoprecipitation. Signal was developed using ECL (GE Healthcare).

From this, in Figure 8, a consistent band around 37 kDa was observed, which is believed to be P0 (uL10), however, we also noticed a strong band around 50 kDa, which is an unexpected result. This 50 kDa band is not detected in our negative control, therefore it is an artefact of the elution. As the negative control is the nuclear fraction, it is anticipated to be blank and see no band as ribosomes are not found in the nucleus. This control was employed to verify the absence of UL10 (P0) within that fraction, thereby confirming the integrity of the separation process. This was successfully done in the META, however, the PCF samples potentially require extra washing steps with a lysis buffer to remove any loosely attached ribosomes. A positive control was not used because it is known that P0 is a stalk protein attached to the ribosome and we were confident that P0 would be detected. However, having a positive control of the purified *T. cruzi* P0 could have helped us identify that the 50kDa band is a byproduct of our experiment. It is speculated that this 50 kDa band could be the Fc region of the heavy chain from the rabbit primary antibody used in our IP since the antibody used in the IP to pull down the ribosomes is the same as the primary antibody used in the western blot. When the IP samples were boiled from the beads in the Laemmli buffer, the antibodies were present. They would have broken down and been loaded onto the gel and were, in turn, detected by the anti-rabbit secondary antibody. Therefore, they could have interfered with the results as the Fc heavy chain is known to be around 50 kDa [48]. Additionally, in Figure 8, no uL10 band is evident in the META 3 blot, even though it is consistent with the other 2 western blots, META 1 and META 2. This could be because the 50 kDa band is highly abundant; its signal may have sequestered the reaction reagent and overpowered the exposure of the uL10 band. The bands in the input were much weaker too, suggesting there were fewer cells in the replicate overall. As a result, it was necessary to verify these western blots using a different secondary approach to determine whether the 50 kDa band was a residual antibody.

To determine whether the band is an antibody artefact, Protein G-HRP conjugate was used instead of HRP-conjugated secondary antibody (Figure 9). The rationale for using HRP-conjugated Protein G is that it does not bind denatured antibodies. As a result, any antibodies boiled and eluted from the beads in the IP should not bind to the Protein G-HRP as they will only bind to the primary antibody of the western blot. It is evident that uL10 has been detected in the samples of both PCF and META as there is a band in the elution (Figure

9). Unfortunately, bands were detected in negative control samples, which could suggest that our cell fractionation was not stringent enough as the negative control is very similar to our input sample in Figure 9 (PCF 2), indicating that the desired separation was not fully achieved. Ultimately, the 50 kDA band was not detected in the Figure 9 western blots and therefore, is a denatured antibody and a Fc heavy chain has a molecular weight of 50kDa [101]. This supports our hypothesis of the antibody artefacts affecting the results.

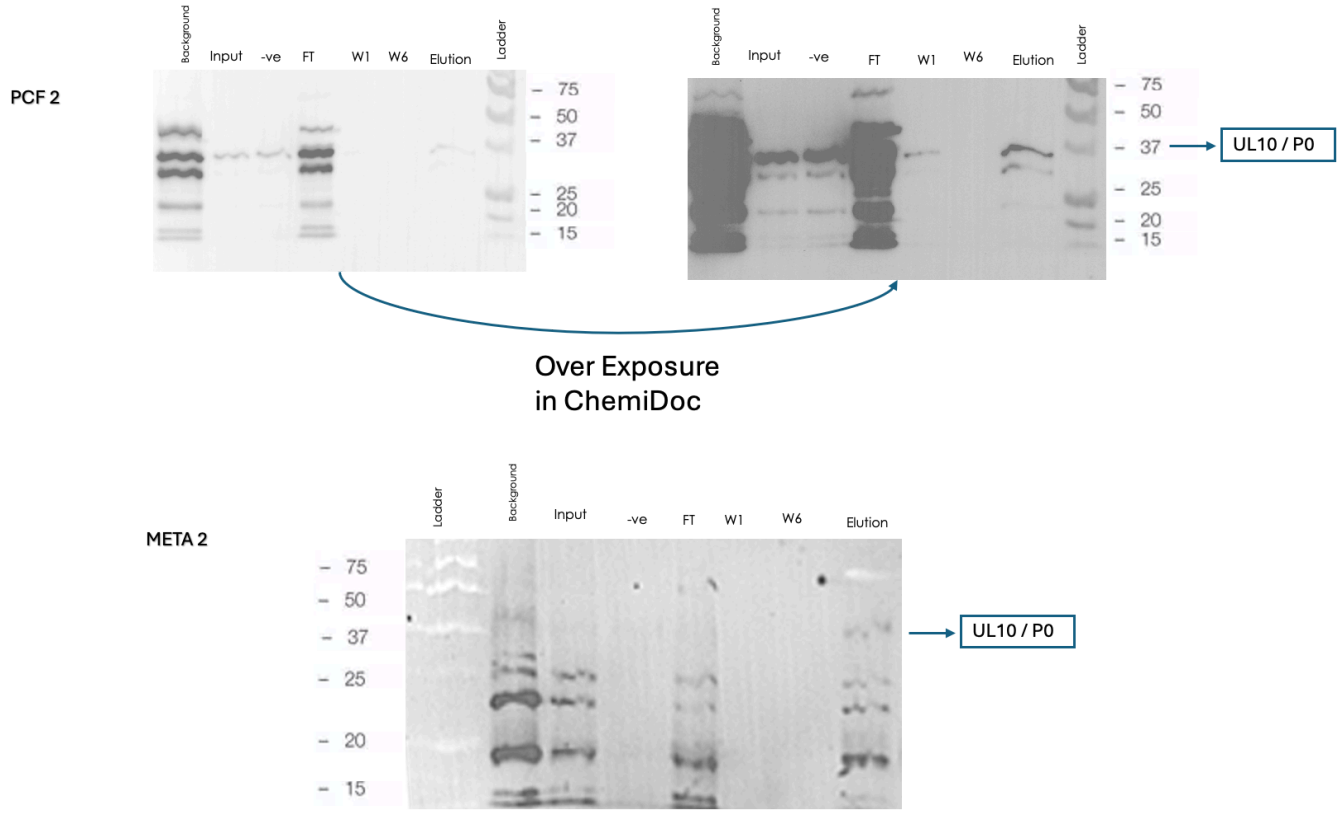

Figure 9: Western blot analysis of PCF 2 and META 2 from Figure 8, but using Protein G-HRP as the secondary. To re-verify the presence of P0 (uL10) with the secondary antibody Protein G-HRP. For the ladder, we used Precision Plus Protein All Blue. The Background is proteins that bind to the Protein A/G beads before antibody incubation, this is the blocking step. The Input is the cytosolic fraction. Negative control (-ve) is the nuclei fraction. FT: flow through, W1: is the first wash, W6 is the last wash, Elution the proteins obtained from the immunoprecipitation. Signal was developed using ECL (GE Healthcare).

3.4 Polysome Profiling Conditions Require Further Optimisation

For our mass spectrometry analyses, we aim to isolate both translating and non-translating ribosomes from *L. mexicana* procyclic (highly proliferative) and metacyclic (quiescent) cells. To ensure that our data represents exclusively proteins that are bound to ribosomes, we specifically wanted to exclude any RNA binding proteins (RBPs) interacting with an mRNA mid-translation. These potential contaminants would co-sediment with polysomes, therefore we decided to evaluate different RNase treatments to digest polyribosomes into monosomes. In this way, mRNA-associated RBPs will not co-sediment with monosomes, or be pulled down by anti-uL10 antibodies. An optimal RNAse treatment strategy would digest mRNA, efficiently converting polysomes into monosomes, whilst keeping degradation of rRNA to a minimum and preserving the structural integrity of ribosomes.

Polysome profiling by sucrose gradient ultracentrifugation is a useful methodology that allows the separation of polysomes, monosomes, ribosome subunits and low-molecular-weight mRNA fragments based on centrifugation properties and their sedimentation rate measured in Svedbergs (S) (Figure 10). The sedimentation rate of any of the ribosomal complexes should be 40 S or greater, with monosomes expected to sediment at 80 S. In this way, we can assess the effects of different RNAse treatments. [49]

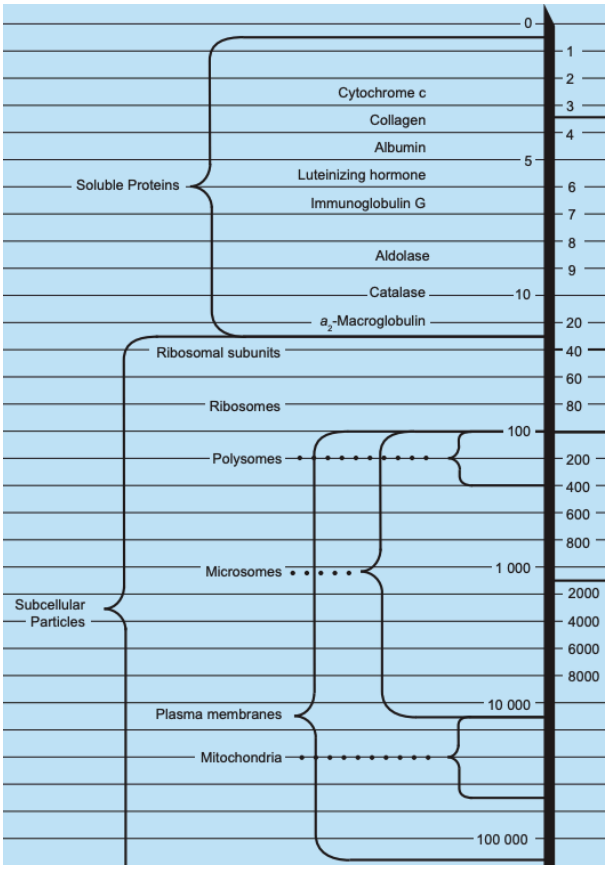

Figure 10: Sedimentation coefficient in Svedbergs of soluble proteins, subcellular particles and biological materials from the Beckman Coulter manufacturer documents [50]

RNase I has been previously used successfully in *T. brucei* and *L. donovani* to isolate and cleave the ribosomes [51], [52]. Therefore, polysome profiling was conducted to evaluate the effect of the RNase digestion to isolate and cleave the ribosomes from the mRNA transcript and to determine whether using RNase I would be more effective than RNAse A. We used PCF cells for these experiments, as they are expected to have a high concentration of ribosomes in a highly proliferative stage. We also used a high concentration of Mg^{2+} in the lysis buffer to prevent dissociation of the 40 S and 60 S ribosomal subunits and thus increase the stability of ribosomes in downstream centrifugation steps [55].

Our polysomal profiling protocol was adapted from published protocols in other eukaryotic species [53]. In brief, live parasites were treated in culture with (CHX) for 10 min to arrest ribosomes in situ. CHX is a translation elongation inhibitor, which binds to the E site of the ribosome [54], this freezes the ribosomes in place and prevents further translation and protein synthesis. This is beneficial for preserving any ribosome-associated proteins and the

core proteins for downstream analysis. These cells were harvested, lysed, cleared of cytoskeletal debris and nuclei and equally split between the controls (RiboLock and SUPERaseIN) and the comparative RNase treatments (RNase A and RNase I). These treatments were followed by a 10-50 % sucrose density gradient centrifugation and a 260 nm UV-light absorbance-based fractionation for detection.

Our first polysome profiling attempt (Figure 11A), was unsuccessful. There were no detectable ribosomes and there were low molecular weight nucleic acids, indicating over-digestion. Therefore, we optimised digestion conditions using different RNase and inhibitors at multiple concentrations and centrifugation speeds. Two different RNases, RNase A and RNase I, are used in this experiment. While RNase I cleaves after all nucleotides and shows no cutting preferences, RNase A is known to be highly biased and will only cleave RNA preferentially after cytosine and uracil pyrimidine residues [53].

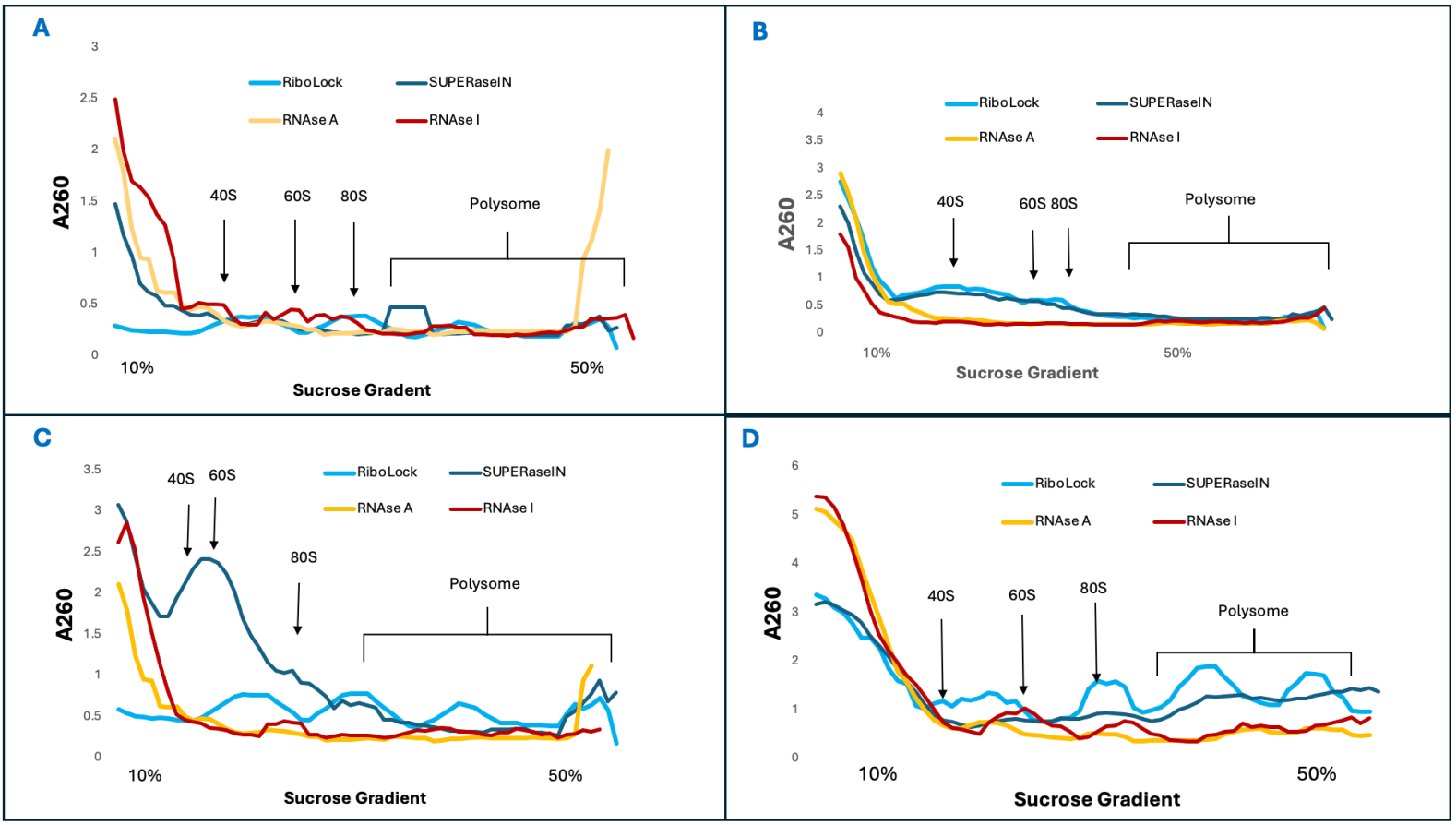

Figure 11: These graphs show the sucrose gradient fractionations of the ribosome. Cells are lysed and loaded onto the top of the gradient which starts at 10% sucrose density. Ultracentrifugation at high g forces causes the separation of mRNA and ribosome complexes. Peaks obtained through the CLARIOSTAR microplate reader (BMG Labtech) measured at 260 nm. Each graph has varying conditions to find which condition would be the most optimal for RNase digestion to separate monosomes from polysomes. RiboLock (light blue), SUPERaseIN (dark blue), RNase A (yellow), RNase I (red),

The conditions:

A) RNase Inhibitor 800 U RiboLock, 100 U SUPERaseIN,
RNase 0.0025 µg/µL RNase A, 1200 U of RNase I
Centrifuge speed of 35,000 rpm /234,500 x g for 3hrs, based on [52], [56].

B) RNase Inhibitor 800 U RiboLock, 200 U SUPERaseIN,
RNase0.00025 µg/µL RNase A, 1200 U of RNase I,
Centrifuge speed 35,000 rpm / 234,500 x g for 3hrs based on [51], [53].

C) RNase Inhibitor 800 U RiboLock, 100 U SUPERaseIN,
RNase: 0.0025 µg/µL RNase A, 1200 U of RNase I,
Centrifuge speed 38,000 rpm / 254,600 x g for 3hrs, repeat of A.

D) RNase Inhibitor: 800 U RiboLock, 100 U SUPERaseIN,
RNase: 0.0025 µg/µL RNase A, 1200 U of RNase I
Centrifuge speed: 31,000 rpm / 210,000 x g for 16hrs (overnight spin), repeat of A but longer spin.

Sucrose gradient analysis revealed no distinct monosomal peaks, indicating complete ribosomal digestion across all RNase treatments (Figure 11), except for in the control (Figure 11C). Subtle peaks observed in control samples suggest partial preservation of ribosomal integrity (Figure 11). Figure 11A shows the initial conditions, based on papers previously published [51], [52], [53], [56]. However, the first attempt was unsuccessful. To optimise the unsuccessful initial experimental conditions, SUPERaseIN concentration was increased and kept constant RNase I to mimic the conditions from [51] and RiboLock were at the same concentrations, whilst RNase A concentration was lowered to try and avoid overdigestion (Figure 11B). This resulted in subtle peaks in the control that suggested some monosomes and polysomes were present that did not separate sufficiently through the gradient. To address this, the treatment conditions were retained and the speed was changed to 38 000

rpm/254,600 x g. The most promising result is shown in Figure 11C, where we see a clear monosome enrichment peak with the SUPERaseIN control (dark blue line).
There were high concentrations of RNA at the start of all the graphs which suggests one of two potential scenarios: 1) Either the sample was not centrifuged sufficiently long enough and was therefore unable to pass through the gradient or 2) everything was being degraded and digested. We opted to try one more repeat (Figure 11D), incorporating an overnight spin while maintaining the same conditions A. This was to ensure that the samples were centrifuged sufficiently and allow everything that could pass through the gradient. Even with an overnight spin, we were unable to isolate monosomes suggesting that varying the centrifugal speeds did not induce a significant difference for the polysome profiling protocol.

We encountered many challenges in isolating monosomes, despite testing with different digestion treatments using RNase A and RNase I at varying concentrations and spin speeds. It was concluded that the treatment regime that was used was too harsh, as the results could indicate the sensitivity of the *L. mexicana* ribosomes and that they are highly sensitive to RNase enzymes. Further optimisation will be required to achieve effective isolation of monosomes without complete ribosome degradation. However, this preliminary data will inform future experimental refinements.

3.5 Bioinformatic Analysis Revealing Protein Activity For Both PCF and META Stages

Although the ribosome profiling experiment revealed substantial ribosomal RNA degradation, the IP samples were still sent to mass spectrometry. These IP samples still provide an opportunity to be able to identify ribosome-associated factors despite challenges with the RNA integrity.

3.5.1 Verifying Mass Spectrometry Data

To identify ribosomal protein compositions, triplicates of PCF and META from the IP for enriched ribosomes (section 3.3) were sent to mass spectrometry. The beads underwent on-bead digestion using the RIME protocol [57] before analysis by PASEF-DIA using an EvoSep One UPLC and Bruker timsTOF mass spectrometer. Ribosomal proteins were analysed by high-resolution mass spectrometry with a filter minimum of 2 unique peptides identified per protein and quantified using peptide precursor ion intensities ($p \leq 0.05$). Mass spectrometry identified over 2000 proteins from the IP samples, with consistent identifications across lifecycle stages. This could be due to over-digestion of the RNase or that the DIA is too stringent. Nonetheless, the samples were consistent between the lifecycle stages, therefore, even with the RNA digest which has degraded the ribosomal RNA we were able to get consistency in the data of proteins for the specific lifecycle stages. This allowed us to identify proteins that are enriched in PCF and META as well as to see if there are any life cycle-specific ribosomal compositions and any potential proteins of interest that play a key role in the parasite's adaptation and differentiation.

3.5.1.1 Principal Component Analysis Revealed Low Variance Between Triplicates

Confirming the integrity of our proteomics, a principal component analysis (PCA) using relative protein quantification derived from unique peptide intensities was used to examine the relatedness between the PCF and META samples and the variability between the replicates (Figure 12). Notably, the triplicate samples cluster within discrete lifecycle stages, displaying low variance among the replicates, especially samples 1 and 2 in both PCF and META. These data suggest the reliability of the results and distinct protein enrichments and protein identities of the specific lifecycle stage.

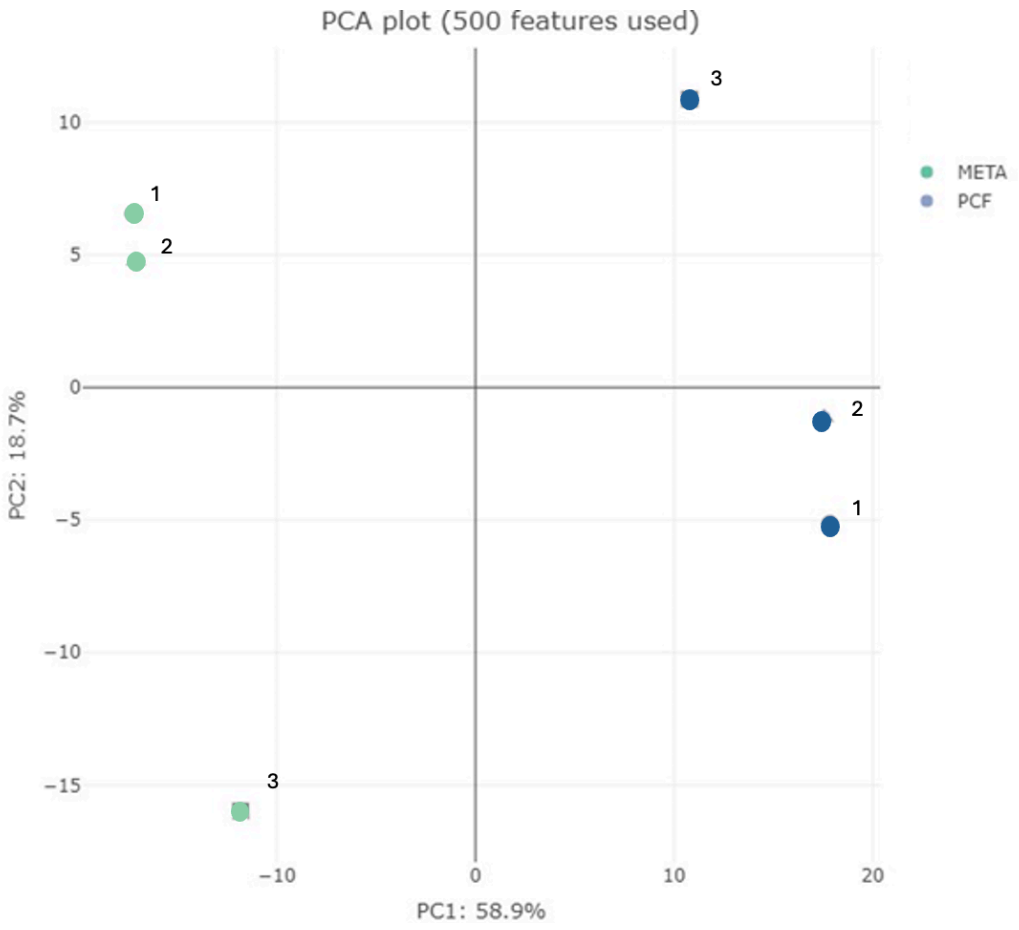

Figure 12: A principal component analysis (PCA) plot that compares the similarities between the PCF triplicates and the META triplicates, made in Frag Pipe Analyst, using relative protein quantification derived from unique peptide intensities was used to examine relatedness between the different biological samples and the variability among replicates. With META in green and PCF in blue. The numbers represent the sample number.

3.5.1.2 Validating Mass Spectrometry Data via Histograms

To ensure validity of the mass spectrometry data, histograms were generated in R to confirm the reliability of the data (Figure 13). A significant deviation should not occur, and a normal distribution curve is expected since the proteins are preserved and play a crucial role in cell survival. The *p*-values and *q*-value were assessed as well. A small *p-value* is strong evidence that there are significant differences in proteins found in META and PCF (Figure 13B), with a substantial amount close to zero. The frequency declines steadily as it approaches closer to 1. The *q-value* (also known as the adjusted *p-value*) is used to filter peptide spectra matches to ensure a certain false discovery rate (FDR), this helps to identify proteins with a high degree of confidence. Due to the large data set the chance of false positives increases, therefore setting the 1% FDR ensures more significance as it reduces the likelihood of false positives. Figure 13C, also has a substantial amount closer to zero; these represent the proteins that are significantly different between META and PCF groups. There is a big peak at 0.2, this could be due to an artefact of the method potentially showing no significance. Therefore the proteins that are closer to zero are strongly significant.

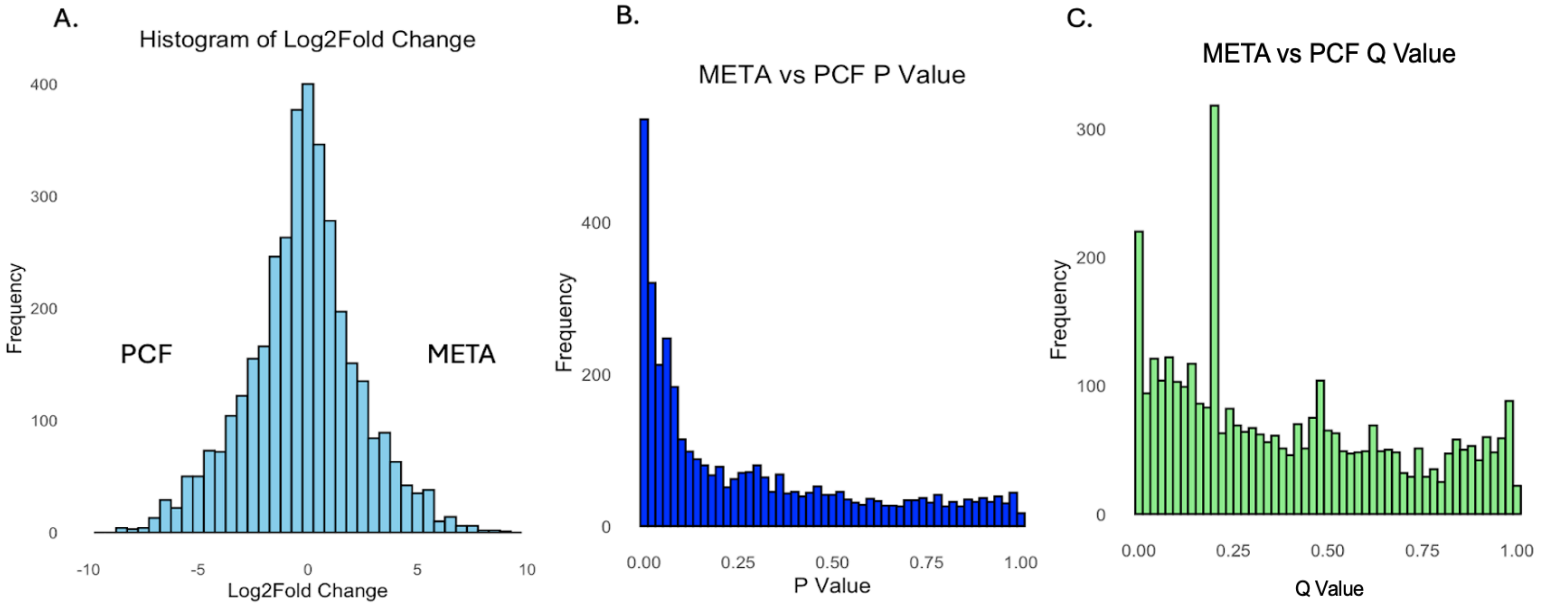

Figure 13: Histograms used to verify whether the data obtained from mass spectrometry is reliable. A) Histogram of Log_2 Fold Change of META vs PCF, with log_2 fold change on the x-axis and frequency on the y-axis and PCF downregulated and META upregulated. B) Histogram of META vs PCF p-value. C) META vs PCF with the adjusted p-value.

3.5.2 Identifying Core Ribosomal Proteins

The mass spectrometry data detected 25% of the core ribosomes from the *L. donovani* ribosome, indicating that we were successful in capturing ribosomes effectively and obtaining core proteins from the large and small subunits (Figure 14). However, we would have expected to have been able to detect all the core proteins as we wanted to enrich ribosomes and ribosomes are conserved molecular machinery, vital for the parasite's survival. However, the mass spectrometry data did also detect a large quantity of mitochondrial ribosomal protein which could have influenced and altered the relative abundance of ribosomal proteins.

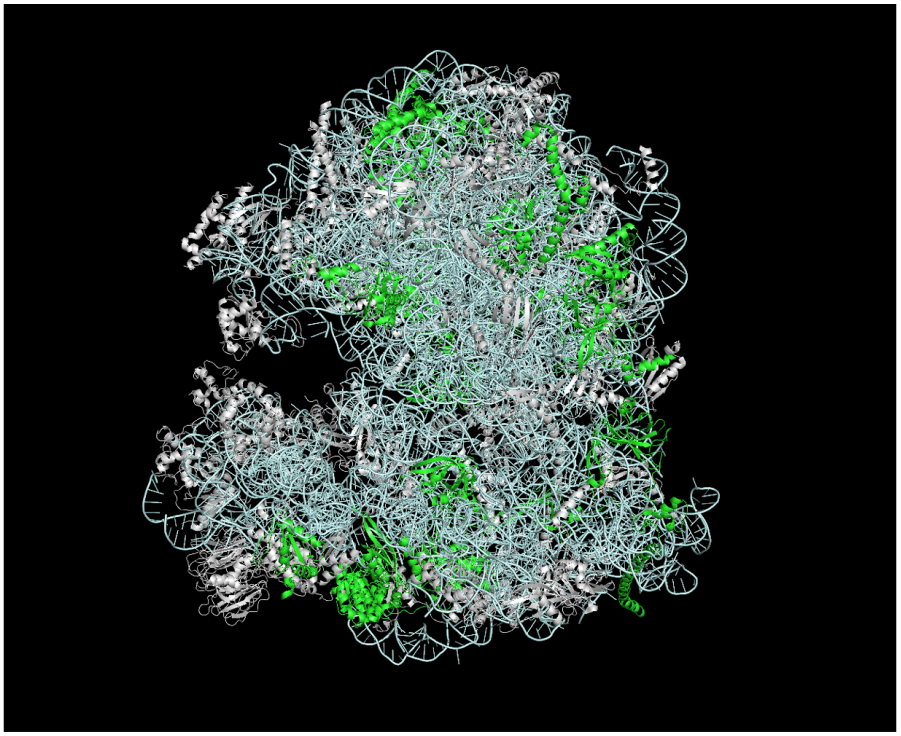

80 S Ribosome

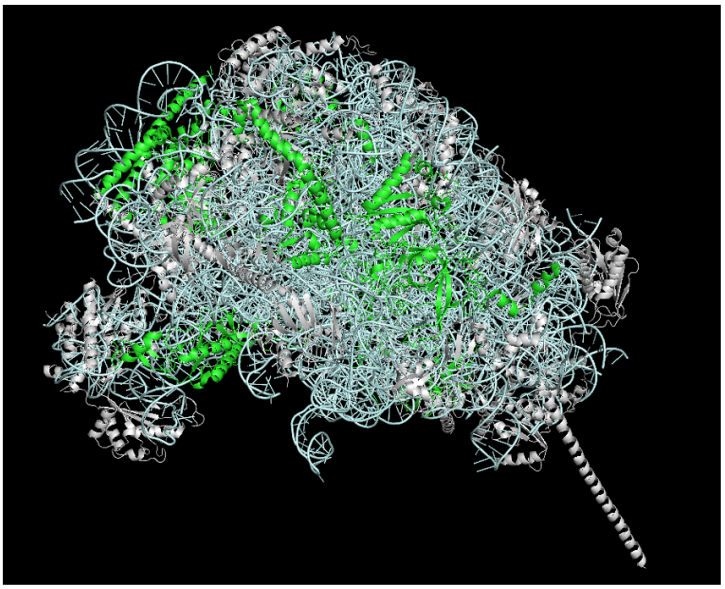

60 S ribosomes subunit

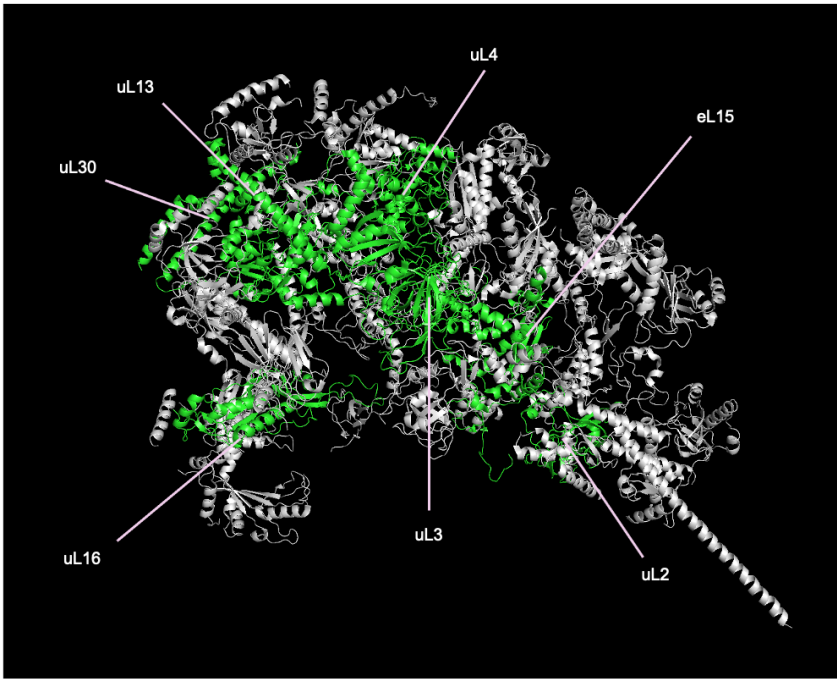

60 S ribosomes subunit, without the structural rRNA

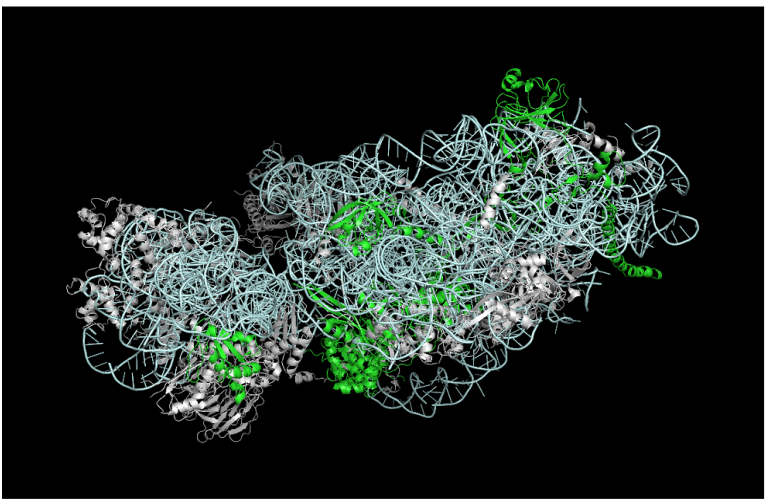

40 S ribosomes subunit

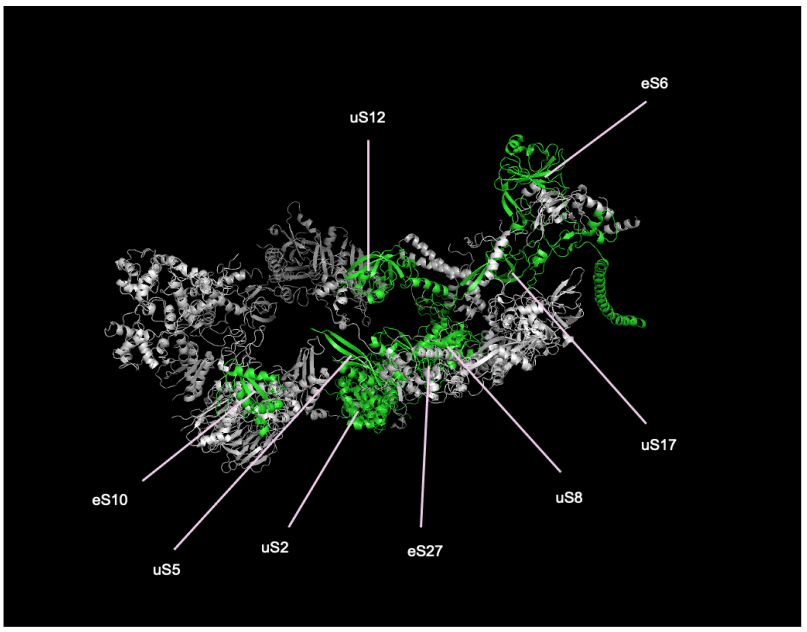

40 S ribosomes subunit, without the structural rRNA

Figure 14: 5T2A shows the core ribosomal proteins identified using mass spectrometry, which have been split into 80 S, 60 S and 40 S subunits for better visualisation. The proteins in cyan are the rRNA structure, green are

the core proteins discovered in our data, while the core proteins in grey were not detected. Figures were produced in PyMol.

It is important to note that *Leishmania* has genes which have the same protein name but can have two or more orthologs (paralogues), which can be seen in Figure 14, this is seen in the entire *Leishmania* and ribosomal proteins are no exception. The paralogous ribosomal proteins in *Leishmania* exhibit compensatory expression; consequently, if one paralogous gene is subject to knockout , the corresponding gene may function as a substitute, maintain protein levels through post-translational mechanisms, and interact with RNA-protein complexes, all of which are critical for effective translation in the parasite, which could help with the parasite adaptation.

3.5.3 Volcano Plot Presenting Significant Stage-Specific Abundant Proteins

The data from the mass spectrometry (Supplementary 1), identified 388 proteins that were statistically significant and differentially abundant between PCF and META samples. These proteins that were selected had a log2 fold change of less than -2 (for PCF) and a log2 fold change greater than 2 (for META), in addition to an adjusted p-value ≤ 0.05 (Figure 15). Data points that are below this significance threshold were excluded. Additionally, only these proteins were differentially abundant in all three replicates, therefore, were considered significant (Figure 15, red dots).

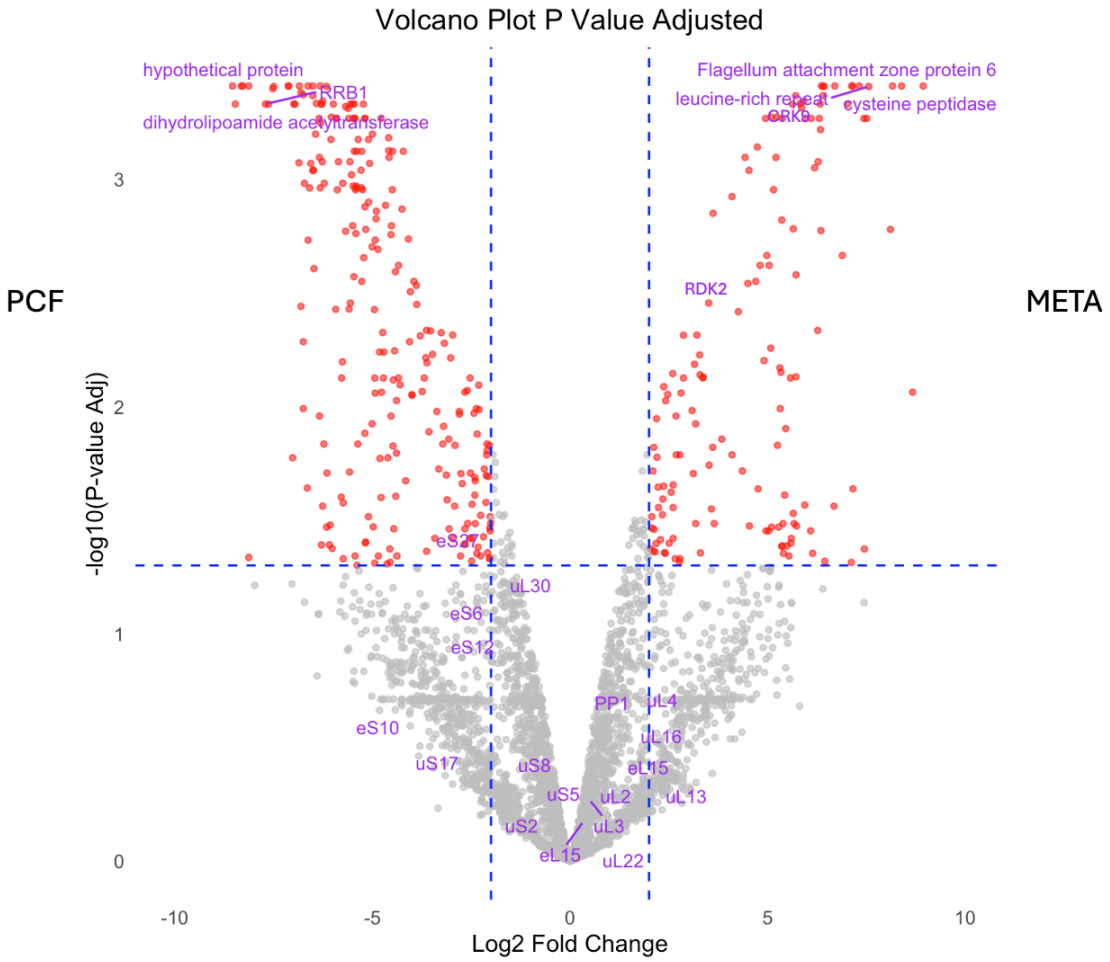

Figure 15: Volcano Plot of the PCF vs META proteins that are enriched from the IP, where the PCF are downregulated, and the META are upregulated. The red dots show the proteins of significance that are differentially abundant and are enriched to the specific life cycle stage, with the left PCF specific and the right META specific. The blue dashed lines represent the cut-off points that the log2 fold changes less than -2 and greater than 2 and the adjusted p-value ≤ 0.05. The proteins in purple are some proteins of interest that will be discussed later on.

Figure 15 reveals the top 3 most significantly differentially abundant proteins found in the mass spectrometry data for META and PCF. As well as the ribosomal subunit proteins detected and some protein kinases and phosphatases which will be discussed in more detail in section 4.1 and 4.2. However, it seems that some of the most significantly differentially abundant proteins are not very specific to ribosome activity, which could suggest that the beads were not fully saturated and may have picked up some non-specific proteins. Aside from RRB1 [102], which is involved in ribosome biogenesis, specifically the assembly of the large 60S ribosomal subunit, this suggests that ribosomal proteins were picked up by the antibodies. Further optimization is needed to ensure the beads are fully saturated to guarantee only translational machinery specific proteins

3.5.4 Venn Diagram of Differentially Abundant Proteins

The Venn diagram (Figure 16), represents total proteins appearing in META and PCF using the Data-independent acquisition (DIA) intensity from Supplementary Data 1, based on the *q* value ≥ 0.05. The DIA intensity is directly proportional to the protein concentration of protein relative to the total protein in the dataset. This is a complementary approach to the volcano plot. We were able to identify which proteins were found specifically in the PCF which were found in META only, however there were some proteins that were found in both PCF and META, suggesting these proteins could be essential for both life cycle stages. The volcano plot fails to recognise shared proteins; for instance, if a protein is detected in both META and PCF, yet the DIA intensity is comparatively higher on the META side than the PCF side, the volcano plot would indicate that it is statistically significant and demonstrates differential abundance in META. However, it does not convey that the protein is also present and downstream in PCF, thereby categorising the protein as “shared”. There is a greater number of total proteins in the Venn diagram than the volcano plot and these also include fragments of overlapping proteins.

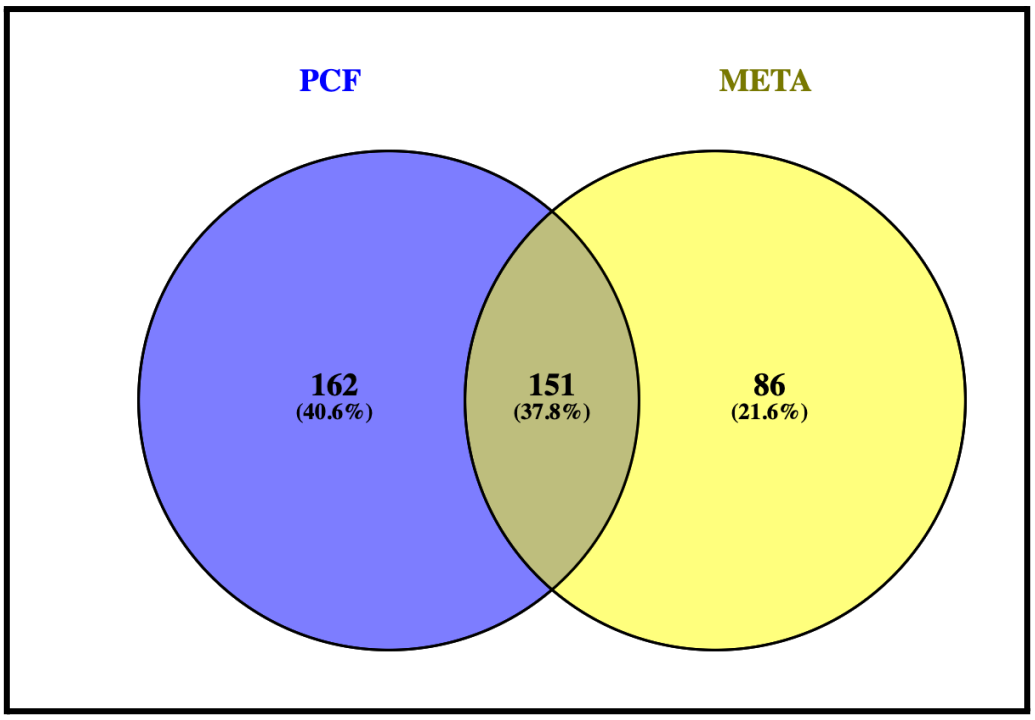

Figure 16: Venn diagram of the significant differentially abundant proteins identified from the mass spectrometry based on the DIA intensity of the three replicates. This highlights proteins that are shared between PCF and META and proteins that are specific to PCF and META only. These proteins are proteins that have an adjusted value of $p \leq 0.05$. Total 399 proteins.

3.5.5 Gene Ontology Term Enrichment

Gene Ontology (GO) considers three distinct aspects of the function of genes and proteins that can help us identify biological processes, cellular locations and molecular functions of the proteins in our data set. GO annotations are associated with specific gene products and help us identify the function of the gene. Biological processes define the biological programs composed of regulated molecular processes. Cellular components define the place where the molecular processes occur in the organism. Molecular functions define the activities at a molecular level.

3.5.5.1 Cytoscape Maps Reveal Significant GO Enrichments

The GO terms were identified in UniProt by using ID mapping. Where the proteins were inputted and UniProt uses its database to identify what GO terms correspond to that specific protein. From this, these proteins were then inputted into the Cytoscape. Cytoscape is designed for biological network visualization, which is based on molecular interactions and

pathways (Kohl, Wiese and Warscheid, 2010). In Cytoscape, the BiNGO application was used. BiNGO is used to determine which GO categories are statistically overrepresented in a set of genes. BiNGO maps the predominant functional themes and outputs this mapping as a Cytoscape graph. The significance is determined by the p value associated with the GO term.

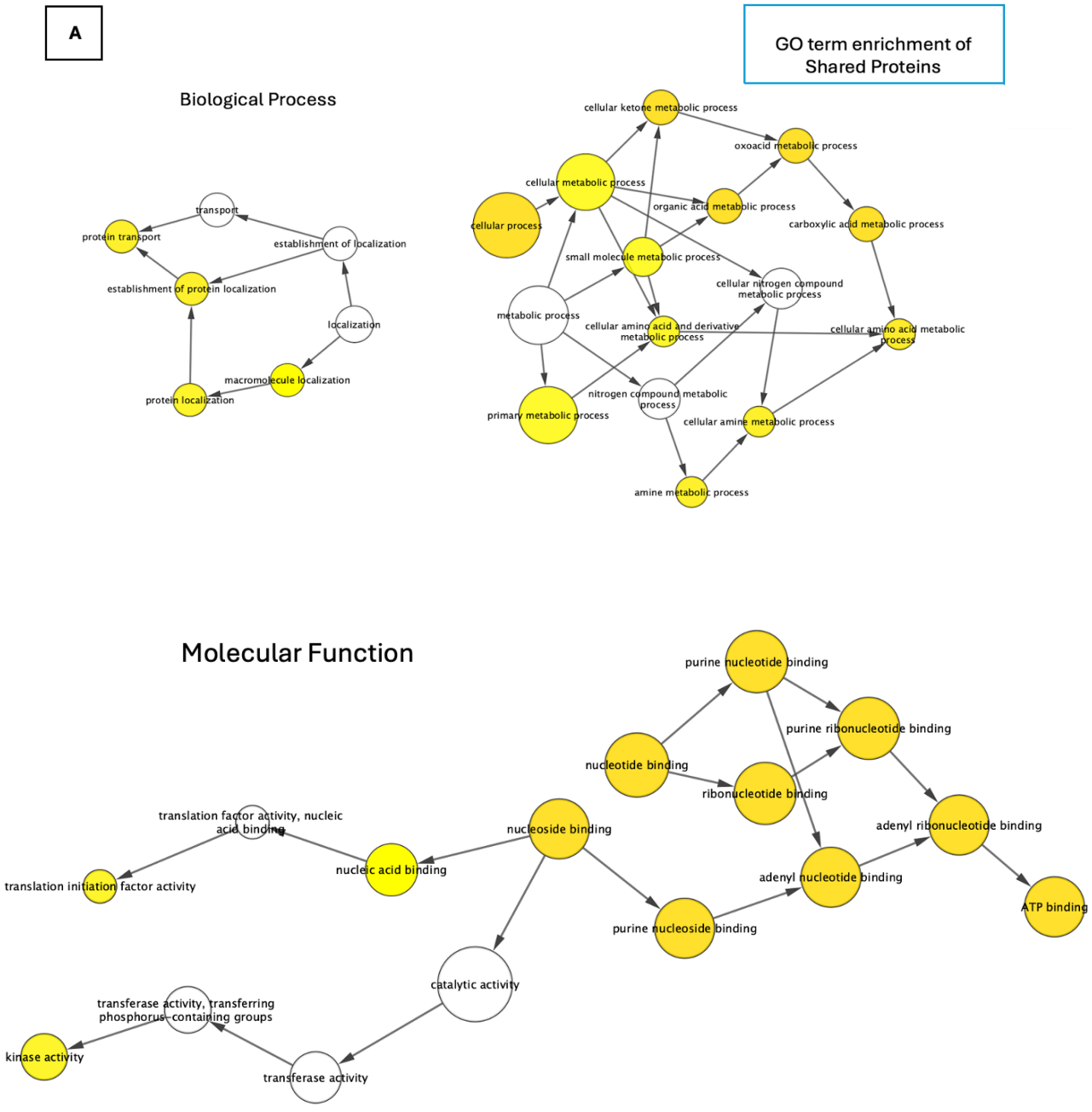

B

Molecular Function

GO term enrichment of PCF specific Proteins

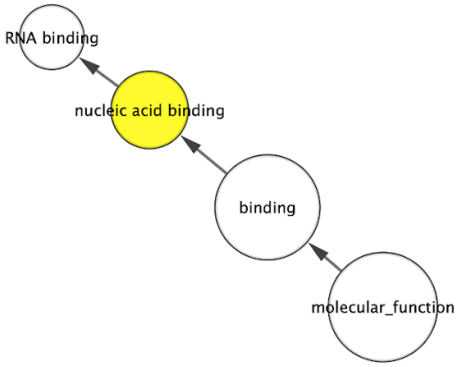

c

GO term enrichment of META specific Proteins

Biological Process

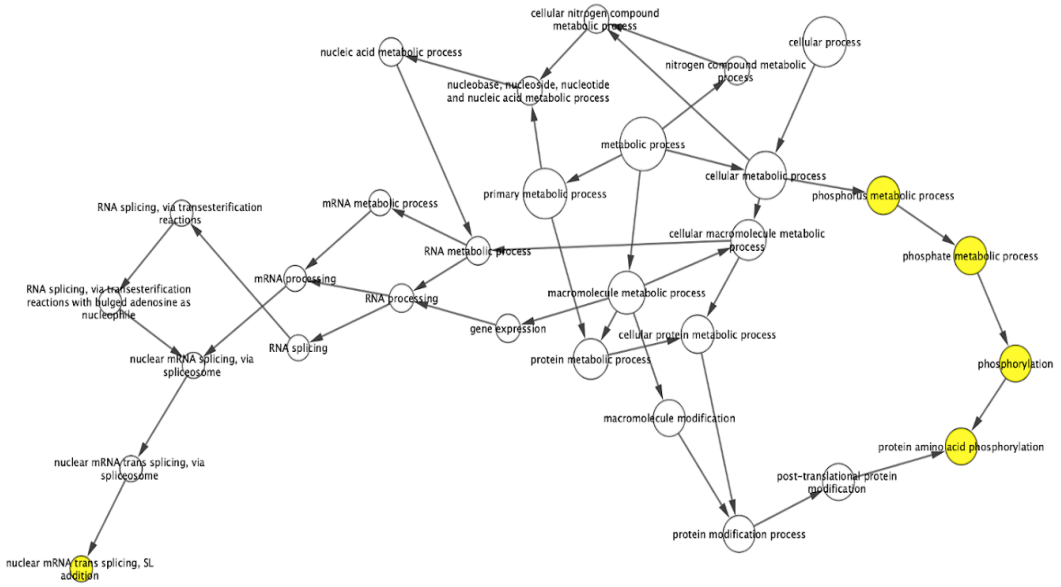

Molecular Function

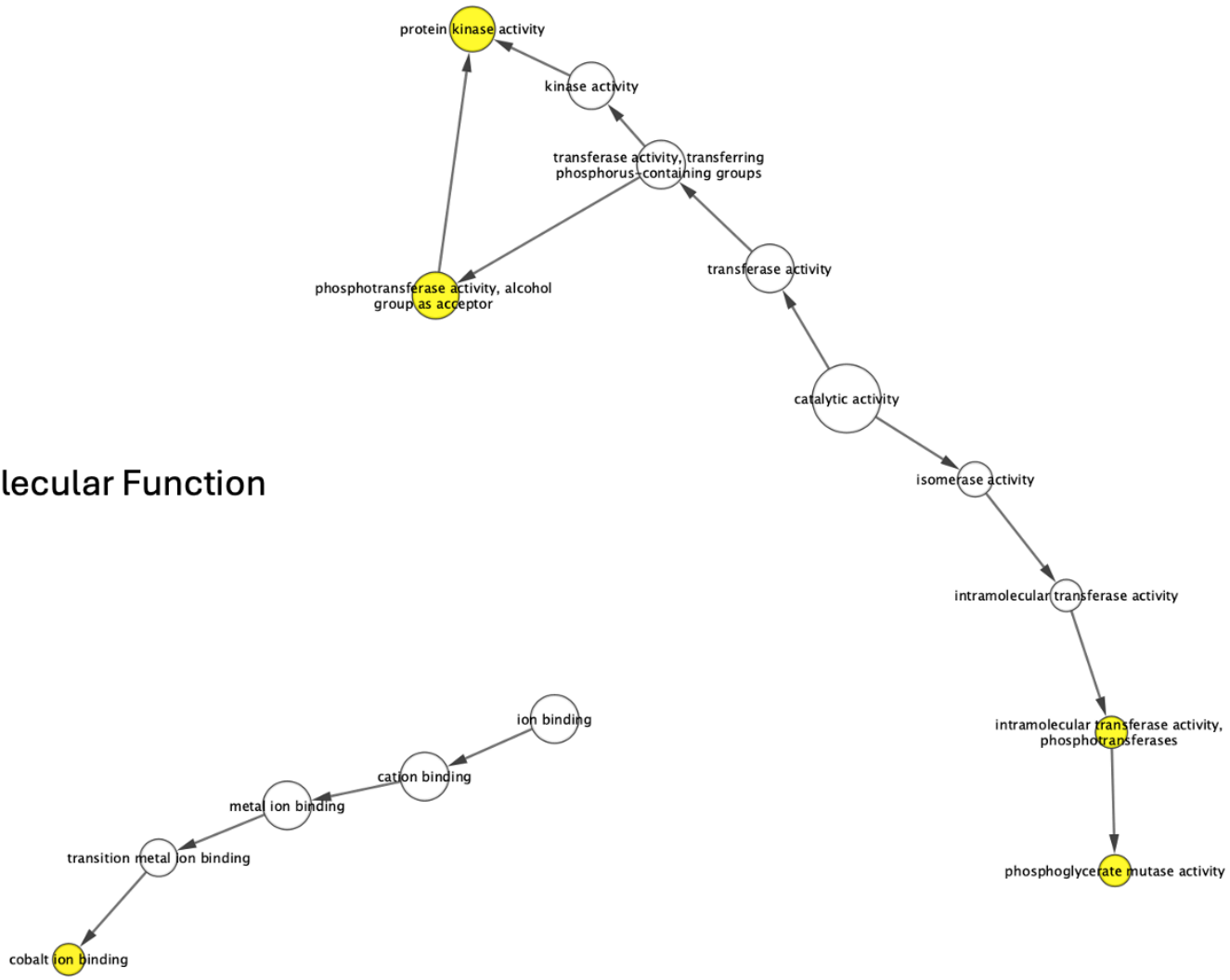

Figure 17: A network of ontology terms where the node colour represents the p-value of the over-represented terms. The Cytoscape graph highlights proteins that are highly abundant in both life cycle stages (PCF and META). The Node (inner circle) size corresponds to the number of genes within the geneset that have that specific GO enrichment term. The colour of the node (inner circle) and border(outer circle) corresponds to the significance based on the BiNGO p-value of the geneset. Yellow represents the GO term p value > 0.05, the darker the yellow the closer to 0 it isThe arrows represent the protein interactions and how they are related to one another.
A) Map of the GO term enrichment of proteins that are significant in both PCF and META, with a p-value threshold of 0.05, presenting the GO terms for their biological processes and their molecular function.
B) Map of the GO term enrichment of proteins that are significant in PCF, with a p-value threshold of 0.1, with only their molecular function.
C) Map of the GO term enrichment of proteins that are significant in META, with a p-value threshold of 0.1, with their biological process and molecular function.

The Cytoscape graph highlights the GO term enrichment of the proteins that are shared in PCF and META. The circles in yellow highlight the significant GO terms based on the threshold applied. These terms are enriched and statistically stand out in comparison to the reference set. The significance threshold for the shared terms is 0.05. From Figure 17A, There is a high representation of nucleotide and ribonucleotide binding which highly suggests ribosome enrichment as they are important for protein synthesis and translation. Metabolic processes also pose as a significant biological process GO that was enriched, as metabolism is essential for the parasite's survival. Protein localisation is important in translation as is essential for transporting proteins in and out of cells.

With a significance threshold of 0.1, PCF-specific proteins show the highest enrichment of nucleic acid binding, implying enrichment of ribosomes or other nucleic acid binding proteins from our IP, Figure 17B. Given that PCF is the most replicative and proliferative stage, it is expected that the nucleic acid binding GO term is significantly enriched as nucleic acid binding plays a critical role in ribosome architecture and protein synthesis.
META-specific proteins with a 0.1 significance threshold revealed a plethora of GO terms, Figure 17C. The significant key terms are phosphorylation-related terms, protein kinase activity and cobalt binding. The differentially abundant proteins, enriched in META phosphorylation and protein kinase activity have played a regulatory role in differentiation.

The reasoning for using 0.05 as a significance threshold for shared proteins was that 0.1 would have resulted in an excessive number of terms at 0.1, therefore a stricter threshold of 0.05 was used to focus on more significant and relevant terms. Whereas for the PCF and META-specific proteins, the stricter threshold of 0.05 yielded too few terms to be able to draw a meaningful conclusion, or none at all for PCF, therefore a more lenient threshold of 0.1 was applied to ensure sufficient data and a better understanding and interpretation of the proteins.

4. Discussion

This project represents a detailed proteomic analysis of two developmental stages of *Leishmania mexicana*, PCF and META promastigote forms relating to their translational machinery. This research builds upon the work of de Pablos *et al.* 2019 [43], which quantitatively analysed the RNA-binding proteome (RBPome) across the life cycle stages of *L. mexicana*. This study highlighted stage-specific heterogeneity in protein expression and RNA-binding capacity, emphasizing the role of trans-regulatory mRNA-protein complexes in parasite life cycle progression. Together, these findings underline the importance of translational regulation in *Leishmania* biology and support the hypothesis that ribosomal components may play a critical role in stage-specific molecular adaptations. However, it is evident that the immunoprecipitation and polysome profiling experiments need to be refined. Once these protocols have been optimised, more in-depth knowledge of conditional variations to the translational machinery could lead to development strategies to block parasite differentiation. This is because differentiation is essential for the parasite's survival in changing environmental stimuli.

The main aspect of this project is isolating and characterising ribosomes from *L. mexicana,* specifically from PCF and META promastigotes. These two stages represent contrasting biological states, with PCF being highly replicative and META entering a quiescent, infective state. Comparing their ribosomal compositions will help identify life cycle-specific molecular components that enable the parasite to alternate between these states. By isolating ribosomal complexes and characterising their components using proteomic approaches, the project aimed to uncover molecular adaptations that enable *Leishmania* to transition between these states and adapt to environmental changes. Additionally, any parasite-specific ribosomal attributes could inform the development of therapeutic strategies targeting *Leishmania's* translational machinery.

Our proteomic analyses have generated new insights into the two developmental stages of the *L. mexicana* translational machinery. Mass spectrometry analysis showed proteins of significance in nucleic acid binding for the PCF proteins, which is expected as the PCF stage is the most proliferative, and many ribosome proteins are bound to rRNA. It also identified several protein kinases enriched in the META stage, including casein kinase and

serine/threonine-specific protein kinases and phosphatase. Gene ontology term enrichment revealed significant upregulation of phosphorylation-related proteins in the META stage, suggesting a key regulatory role for these proteins during this life cycle transition. Notably, the absence of these proteins in the PCF suggests that they could play a role in the META's quiescence and virulence. Previous studies have shown that phosphorylation modulates ribosomal assembly and stress responses in kinetoplastids, supporting our findings [58], [59]. This phosphorylation may fine-tune translational regulation, enabling the parasite to adapt to nutrient-limiting conditions encountered during host infection.

4.1 The Role of Phosphorylation in Translation Regulation

Protein post-translational modifications (PTM) are one of the most important mechanisms to regulate proteins. Protein phosphorylation plays a central role in almost all aspects of cellular processes and has been shown to regulate protein function, stability and turnover rate [60]. Regulation of this specific activity appears to be a general mechanism for the control of protein synthesis and plays a role in modulating translation [61]. The majority of phosphoproteins identified are known to be differentially regulated between promastigotes and amastigotes, with more phosphorylation in the latter stage in AMA [62]. Our mass spectrometry data (Supplementary Data 1) identifies known *Leishmania* phosphoproteins previously described by Rosenzweig *et al*. 2008 [60], thus providing an independent validation of our results. In addition, the microtubule-associated protein showed a similar increase in phosphorylation, indicating that these modifications may be linked to cytoskeletal remodelling during differentiation, especially when the META changes from an elongated cone shape to an oval shape to form the AMA structure (Figure 1).

Phosphorylation can regulate translation and enable the response to environmental changes. By modulating protein synthesis, cells can adapt to various stimuli, ensuring the correct proteins are being produced, which is essential for maintaining homeostasis and responding to stress [63]. This notion also supports the fact that protein phosphorylation plays an important role during *Leishmania* differentiation and this process is likely controlled by stage-regulated protein kinases and phosphatases, which is consistent with our data in Figure 17 C as we have significant GO terms of phosphorylation and protein kinases. Phosphorylation and dephosphorylation events likely constitute a regulatory pathway

controlling *Leishmania* differentiation. Phosphorylation has activation and suppressive characteristics, therefore would play a big role in the quiescence stage of the META. The transient changes in protein phosphorylation contribute to similar changes in mRNA and protein abundance observed during differentiation [64].

In *Leishmania*, phosphatases are involved in adapting to different environments and stress conditions, which is vital for the survival and virulence of the parasites. Studies have shown that several phosphatases are upregulated in metacyclic promastigotes, such as serine/threonine phosphatases. This can help the parasites adapt to stress conditions and are involved in their differentiation and virulence. This upregulation of phosphatases is believed to enhance the parasites' ability to infect the host and evade the immune response and is linked to the parasites' ability to adapt to the harsh conditions they encounter in the mammalian host [65].

There are a few protein phosphatases that are known to be in *Leishmania* [65], [85], [88] . Protein phosphatase 5 (PP5) has the greatest protein expression in META compared to all the other cycle stages suggesting its importance for metacyclogenesis [85]. PP5 has a dual function where it dephosphorylates substrates and also co-chaperones under stress response [86]. Phosphatases can also help modulate the host's immune response, allowing the parasites to survive and proliferate within macrophages. For instance, protein phosphatase 1 (PP1) has immunomodulatory effects on the host cell. This enables the survival of the parasite within the host [85]. PP1 is also known to inhibit replication and cell cycle division, which links to the META quiescent state [88]. Overall, the correlation between META promastigotes and phosphatases is significant, as the upregulation of these enzymes in the infective stage plays a crucial role in the parasites' adaptation, survival, and virulence during infection [65]. PP1 is found in our Supplementary Data 1, known as LmxM.33.0790. Our data shows that it is only found downstream in the META stage, which is consistent with the literature.

It is well established that the phosphorylation of proteins is involved in all major steps of translation, including translation factors, the control and regulation of the performance of the translational machinery and, consequently, the cellular proteome [66]. A notable example is the phosphorylation of eIF2α by the Gcn2 kinase, which is activated during the Integrated Stress Response pathway [67]. This phosphorylation event inhibits the translation

of housekeeping mRNAs while promoting the translation of stress-adaptive mRNAs [79]. A similar mechanism could explain the entry of META promastigotes into quiescence. The changes in pH and temperature encountered during the transition to the host environment may activate a stress response pathway, leading to increased phosphorylation activity that downregulates translation. This adaptive mechanism could allow the parasite to conserve resources and prepare for the next stage of its life cycle.

4.2 The Role of Protein Kinases in Translation Regulation

Protein Kinases are enzymes that catalyse the transfer of phosphates of ATP to protein substrates which in turn alters the function of the protein [68]. Our mass spectrometry analysis revealed the enrichment of protein kinases that were also found in Baker *et al*., 2021 [69]. These protein kinases: cdc2-related kinase (CRK9) and repressor of differentiation kinase 2 (RDK2), were revealed to be significantly abundant in the META stage, figure 15.

LmxM.27.1940 (CRK9) has a dual role that controls the cell cycle and is a critical regulator in gene expression. Our identification of CRK9 in META is consistent with studies in *T. brucei,* where it also revealed direct interaction with the ribosomal protein L5 [70]. The silencing of CRK9 resulted in a strong decline of mature mRNA levels accompanied by an increase in unspliced pre-mRNA in the *T. brucei* procyclic and bloodstream forms [70]. Additionally, the silencing of CRK9 also caused the loss of RBP1 phosphorylation. The loss of phosphorylation can cause protein defects in the recruitment of splicing factors and alter the splicing pattern, strongly indicating a direct role of CRK9 in RNA splicing [70]. This protein kinase is found specifically in META and is significantly abundant. The role of CRK9 in RNA splicing suggests a potential link between stage-specific phosphorylation and the regulation of ribosome-associated transcripts during life cycle transitions.

LmxM.30.2960 (RDK2) is a serine/threonine kinase, crucial for regulating various cellular functions. Including the cell cycle, which is involved in the series of events that lead to cell division and replication. This regulation is essential for the parasite's ability to multiply and transition between different forms during its life cycle. The kinase activity of RDK2 helps ensure that the parasite can progress through its life cycle stages effectively, which is vital for its survival and propagation [70]. This protein kinase is also significantly abundant and it is found in both PCF and META but the protein abundance level in the META life cycle stage is

significantly greater than in the PCF life cycle stage. Though RDK2 does not directly bind to the ribosome, this protein kinase may indirectly regulate translation. The significant enrichment of RDK2 in the META stage aligns with the need for precise post-transcriptional regulation, suggesting its importance in controlling the parasite's adaptation to the host environment.

Protein kinases are key for cell cycle regulation, with specific phosphorylation events necessary for their activity and differentiation in *T. brucei* [72], there is also an indication that protein kinases are likely significant players in controlling mRNA turnover, which is essential for modulating gene expression in *T. brucei, T. cruzi* and *Leishmania* parasites [73]. It is interesting to note that PP1 in *T. brucei* may regulate cdc2-related kinases that promote cytokinesis [88], indicating how interconnected pathways are and providing confidence in these proteins having a relationship within translation. Survival and virulence in *Leishmania* involve protein kinases as well, as they regulate parasite viability, including cell-cycle progression and differentiation, making them vital for the parasite's life cycle [74], emphasising how important these protein kinase activity and phosphorylation events are important, not just in the ribosome but for the parasite as a whole, these are particularly important in the complex life cycle and environmental adaptation of kinetoplastids.

4.3 Experimental Review and Troubleshooting

Immunoprecipitation experiments showed that ribosomes were enriched and some significant data was obtained. However, we get a very low protein abundance of P0/uL10 protein in the elution in comparison to all the other proteins detected in the input sample and the flow through (Figures 8 and 9). It is expected that if we were to specifically enrich ribosomes we would see a major uL10 band, proportional to the number of ribosomes that were captured on the surface of the beads. One possible explanation is that the beads were not saturated with enough antibody molecules to achieve maximum ribosome enrichment, as the antibody dilution used was 1:1000. This could suggest why only 25% of core ribosomal proteins were detected (Figure 14). To optimise the enrichment of the ribosomes, we must ensure that the Protein A/G beads are fully saturated with the antibody and that all of the antibodies occupy and bind to the Protein A/G bead sites. We used 2.0 mg per 100 µl of beads for every sample, the binding capacity of IgG for the beads is 0.4 - 0.5 mg/ml,

therefore in 100 µl beads the binding capacity is 40 - 50 µg. The concentration of the P0 antibody was assessed on the Nanodrop, with a PBS blank, as the original concentration is unknown. From this, it is calculated that a ~ 1:300 dilution of antibodies is required to fully saturate 0.04 mg of Protein A/G beads. In Figures 8 and 9, we also observe P0-related proteins in the 'background' lane, this shows that our blocking step worked and that the beads will bind to non-specific proteins. However, it is very unlikely that all the non-specific proteins were collected in the blocking step, and due to the beads not being fully saturated by the P0 antibody, they could have bound to the beads even after the blocking step. As a control for our mass spectrometry, we should have sent the background bead samples for analysis and then removed these non-specific proteins from our data set to get a clearer result and more confidence that our data are ribosome-associated proteins and not proteins that happen to bind to the beads, which could be the reasoning of having over 2000 and some replicates with over 3000 proteins in our dataset. However, the over-digestion of the RNA may have also caused issues with the data and therefore optimisation of the RNA digestion is also required.

Polysome profiling is a versatile technique that can be used to examine ribosomes and any ribosome-associated proteins, especially in *Leishmania,* where transcriptional control is greatly absent and gene expression regulation mainly occurs during translation [12]. Many studies have conducted ribosomal profiling experiments on various classic eukaryotes [53], however, there are very few ribosome profiling for *Leishmania* and even less for *L. mexicana. Leishmania spp.* are ancient eukaryotes and have diverged from the other eukaryotes quite early on. The phylogenetic tree (Figure 18) depicts the relationship between the *Leishmania spp.* and the other eukaryotes, including mammals, plants and yeast. The group of protozoa have diverged very early from the eukaryotic lineage, and are a compelling model to study the variability of highly conserved processes such as protein translation. As identified, *Leishmania* has highly diverged from humans and other opisthokonts. As a result, we designed and developed a protocol to compare two different types of RNase: RNase A and RNase I, as well as RNase inhibitors: RiboLock and SUPERaseIN, to determine which enzyme will cleave the mRNA but leave rRNA and ribosomes intact. This would allow us to optimise the number of monosomes for the cell fractionation experiment while avoiding complete digestion. Assessing the sucrose gradients, it observed that the ribosomes had been

completely digested which suggests that too much RNase was added as we can see subtle peaks in the controls (Figure 11). Unfortunately, in this study, we were unable to optimise this ribosomal profiling protocol as we see no significance between the different inhibitors or RNases. There are many potential reasons why this might be. It could be that the treatments used here were too harsh for *Leishmania* ribosomes, or it could suggest that the *Leishmania* ribosomes are very sensitive in comparison to other eukaryotic or unicellular organisms. It could also suggest that the endogenous RNase could be very potent and therefore our inhibitor concentration is not enough to quench the RNase activity that is in the parasites in the first place.

Although other papers have successfully used the UV lamp fractionator [53], [75], [76], it was unavailable during the time of the experiment. Instead, we split the sucrose gradient manually into a 96 well UV-transparent plate and measured the absorbance at 260 nm. This method worked for Sobhany *et al,* 2021 and we followed similar procedures [77]. However, fractions must be gathered without interfering with the remainder of the gradient, and all fractions must have the same volume. Manual pipetting is not as accurate as using a fractionator, therefore human error is a possibility.

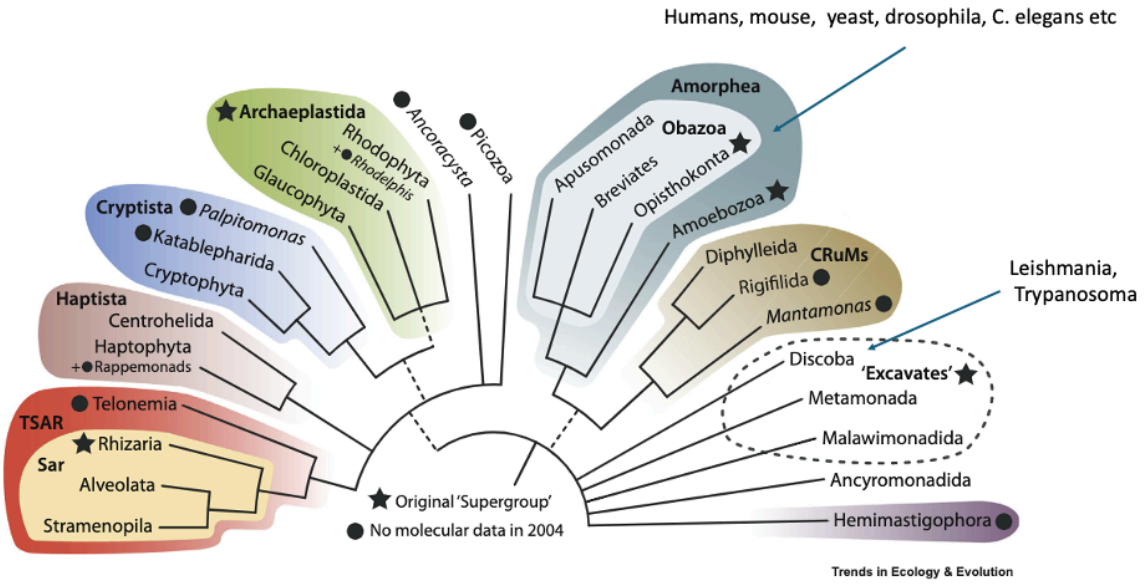

Figure 18: Phylogenetic Tree of Eukaryotes [80]. Annotated with humans, mice, yeast, *drosophila*, C. *elegans* etc., *Leishmania* and *Trypanosoma*, to emphasise the distinctions between different species. This is a summary based on a consensus of recent phylogenomic studies. The coloured groupings correspond to the current 'supergroups'.

A ribosome profiling study by Bifeld *et al*., 2018 [52] digested *L. donovani* polysomes using RNase I, followed by quenching with RNaseIN as the inhibitor. However, RNase I can only be inhibited by SuperaseIN, while RNase A is compatible with a wider range of commercially available RNase inhibitors. Therefore, this study is not reliable as RNaseIN does not effectively quench RNase I, it is known to only inhibit RNase A, B and C [78]. RNase A has worked successfully for limited RNase digestion in many eukaryotes [53], [56], [66] and can be inhibited with a broad range of RNAse inhibitors. We wanted to compare which out of RNase A and RNase I would work better in cleaving RNA and help us successfully isolate ribosomes. As *Leishmania* is a unicellular organism we expect to see similar outcomes with *E. coli* and *S. cerevisiae* as they are also unicellular organisms [53]. We based our protocol predominately on the *T. brucei* paper [51] as it was the closest species to *Leishmania* and had distinct monome peaks, indicating that their polysome profiling was successful, whereas the *L. donovani* paper [52] proved to be unreliable. They did not use the correct inhibitor for their RNase and their results did not show distinct monosomal peaks, consistent with our data in which ribosomes are being digested. Unlike the results observed in *T. brucei* where distinct monosome peaks were obtained, our findings suggest that *Leishmania* ribosomes may be inherently more sensitive to RNase treatments. This could reflect ribosomal composition or structural integrity differences between these kinetoplastid species.

4.4 Future Studies

Further studies, including phosphoproteomics and functional characterization of key kinases, are needed to validate these findings and uncover the specific mechanisms linking phosphorylation to ribosomal regulation in *Leishmania*. The immunoprecipitation and RNase digest protocols should be further optimised before conducting additional experiments, such as cell fractionation, in which the ribosomes are pelleted through a sucrose cushion. Ideally, the RNase digest should preserve the ribosomes while eliminating any background proteins that could cause ‘noise’ in the mass spectroscopy. Had we been able to optimise RNAse treatment conditions, this experiment would have provided an alternative enrichment method. It would be interesting to see whether any additional proteins might be detected in the ribosome pellet that was absent in the immunoprecipitation. After that, it would be wise

to also endogenously tag P0 in the parasite with a high-affinity epitope tag, via CRISPR/Cas9 tagging to additionally validate findings. This would allow for the use of commercial antibodies, more stringent washes and therefore more accurate identification of proteins that would bind to the ribosome. It is important to note that although the DIA intensity contains blanks, this does not imply that no proteins were found; rather, it mostly indicates that the amount of proteins found was below the significance threshold, which could distort the results. Once we have greater confidence in the proteins detected, structural techniques such as cryo-EM would be useful to further investigate stage-specific variation in ribosome composition. Cryo-EM has the potential to advance our understanding of ribosomal dynamics, and mechanisms of ribosome-binding proteins. This could provide insights into variations in ribosomal structures across different strains and species. This could lead to a better understanding of how these differences affect ribosomal function in specific life-cycle stages.

The study highlights the importance of translational regulation in *Leishmania* life cycle transitions. Our findings provide novel insights into the stage-specific ribosomal adaptations and phosphorylation-related processes and how the parasite modulates gene expression in response to environmental stimuli, laying the groundwork for targeted interventions against this parasitic disease.

References

1. Edoardo Torres-Guerrero, Marco Romano Quintanilla-Cedillo, Ruiz-Esmenjaud J, Arenas R. Leishmaniasis: a review. F1000Research [Internet]. 2017 May 26 [cited 2024 Oct 5];6:750–0. Available from: https://www.ncbi.nlm.nih.gov/pmc/articles/PMC5464238/

2. Guarnizo A, Tikhonova EB, Karamyshev AL, Muskus CE, Karamysheva ZN. Translational reprogramming as a driver of antimony-drug resistance in Leishmania. Nature Communications [Internet]. 2023 May 5 [cited 2024 May 27];14(1). Available from: https://www.nature.com/articles/s41467-023-38221-1

3. WHO. Leishmaniasis. Whoint [Internet]. 2023 Jan 12 [cited 2024 Dec 27]; Available from: https://www.who.int/news-room/fact-sheets/detail/leishmaniasis

4. World Health Organization. Global leishmaniasis surveillance updates 2023: 3 years of the NTD road map [Internet]. Who.int. World Health Organization; 2024 [cited 2024 Dec 27]. Available from: https://www.who.int/publications/i/item/who-wer-9945-653-669

5. WHO. W.H.O. Global leishmaniasis update, 2006–2015: a turning point in leishmaniasis surveillance. WHO Weekly Epidemiology. 2017;Rec. 2017; 92:557-572.

6. Feliciangeli MD. Natural breeding places of phlebotomine sandflies. Medical and Veterinary Entomology [Internet]. 2004 Mar 1 [cited 2024 Dec 27];18(1):71–80. Available from: https://resjournals.onlinelibrary.wiley.com/doi/10.1111/j.0269-283X.2004.0487.x

7. Stanley AC, Engwerda CR. Balancing immunity and pathology in visceral leishmaniasis. Immunology and Cell Biology [Internet]. 2006 Dec 5 [cited 2024 Oct 4];85(2):138–47. Available from: https://onlinelibrary.wiley.com/doi/10.1038/sj.icb7100011

8. Sébastien Besteiro, Williams RAM, Coombs GH, Mottram JC. Protein turnover and differentiation in Leishmania. International Journal for Parasitology [Internet]. 2007 Apr 2 [cited 2024 Dec 27];37(10):1063–75. Available from: https://pmc.ncbi.nlm.nih.gov/articles/PMC2244715/

9. Ambit A, Woods KL, Cull B, Coombs GH, Mottram JC. Morphological Events during the Cell Cycle of Leishmania major. Eukaryotic Cell [Internet]. 2011 Sep 17 [cited 2024 Oct 22];10(11):1429–38. Available from: https://pmc.ncbi.nlm.nih.gov/articles/PMC3209043/

10. Gluenz E, Höög JL, Smith AE, Dawe HR, Shaw MK, Gull K. Beyond 9+0: noncanonical axoneme structures characterize sensory cilia from protists to humans. The FASEB Journal [Internet]. 2010 Apr 6 [cited 2024 Oct 22];24(9):3117–21. Available from: https://pmc.ncbi.nlm.nih.gov/articles/PMC2923350/

11. Kloehn J, Saunders EC, O'Callaghan S, Dagley MJ, McConville MJ. Characterization of Metabolically Quiescent Leishmania Parasites in Murine Lesions Using Heavy Water Labeling. PLoS Pathogens [Internet]. 2015 Feb 25 [cited 2024 Oct 23];11(2):e1004683–3. Available from: https://pmc.ncbi.nlm.nih.gov/articles/PMC4340956/

12. Karamysheva ZN, Gutierrez A, Karamyshev AL. Regulation of Translation in the Protozoan Parasite Leishmania. International Journal of Molecular Sciences [Internet]. 2020 Apr 23 [cited 2024 Dec 27];21(8):2981–1. Available from: https://pmc.ncbi.nlm.nih.gov/articles/PMC7215931/

13. Pimenta P, Turco S, McConville M, Sacks D, Perkins P, Lawyer PG. Science New Series. Vol. Vol. 256, No. 5065. American Association for the Advancement of Science; 1992.

14. Bates P, Rogers M. New Insights into the Developmental Biology and Transmission Mechanisms of Leishmania. Current Molecular Medicine [Internet]. 2004 Sep 1 [cited 2024 Dec 27];4(6):601–9. Available from: https://pubmed.ncbi.nlm.nih.gov/15357211/

15. Peters N, Sacks D. Immune privilege in sites of chronic infection: *Leishmania* and regulatory T cells. Immunological Reviews [Internet]. 2006 Sep 14 [cited 2024 Oct 15];213(1):159–79. Available from: https://onlinelibrary.wiley.com/doi/full/10.1111/j.1600-065X.2006.00432.x

16. Cohen-Freue G, Holzer TR, Forney JD, McMaster WR. Global gene expression in Leishmania. International Journal for Parasitology [Internet]. 2007 May 9 [cited 2024 Oct 15];37(10):1077–86. Available from: https://www.sciencedirect.com/science/article/pii/S0020751907001348

17. Cooper GM. Translation of mRNA [Internet]. Nih.gov. Sinauer Associates; 2024 [cited 2024 Oct 21]. Available from: https://www.ncbi.nlm.nih.gov/books/NBK9849/

18. Liu Z, Gutierrez-Vargas C, Wei J, Grassucci RA, Ramesh M, Espina N, et al. Structure and assembly model for the *Trypanosoma cruzi* 60S ribosomal subunit. Proceedings of the

National Academy of Sciences [Internet]. 2016 Oct 10 [cited 2024 Sep 17];113(43):12174–9. Available from: https://www.ncbi.nlm.nih.gov/pmc/articles/PMC5087005/

19. Raman AV, de G, Kusebauch U, Pan M, Serdar Turkarslan, Moritz RL, et al. Context-Specific Regulation of Coupled Transcription-Translation Modules Predicts Pervasive Ribosome Specialization. SSRN Electronic Journal [Internet]. 2018 Jan 1 [cited 2024 Oct 24]; Available from: https://papers.ssrn.com/sol3/papers.cfm?abstract_id=3155765

20. Blanchet S, Ranjan N. Translation Phases in Eukaryotes. Methods in Molecular Biology [Internet]. 2022 [cited 2024 Oct 21];217–28. Available from: https://www.ncbi.nlm.nih.gov/books/NBK586875/

21. Cheung YN, Maag D, Mitchell SF, Fekete CA, Algire MA, Takacs JE, et al. Dissociation of eIF1 from the 40S ribosomal subunit is a key step in start codon selection in vivo. Genes & Development [Internet]. 2007 May 15 [cited 2024 Oct 21];21(10):1217–30. Available from: https://pmc.ncbi.nlm.nih.gov/articles/PMC1865493/

22. De Gaudenzi JG, Jäger AV, Ronan Izcovich, Campo VA. Insights into the Regulation of mRNA Processing of Polycistronic Transcripts Mediated by DRBD4/PTB2, a Trypanosome Homolog of the Polypyrimidine Tract‐Binding Protein. Journal of Eukaryotic Microbiology [Internet]. 2015 Dec 14 [cited 2024 Oct 25];63(4):440–52. Available from: https://onlinelibrary.wiley.com/doi/10.1111/jeu.12288

23. Clayton C. Regulation of gene expression in trypanosomatids: living with polycistronic transcription. Open Biology [Internet]. 2019 Jun 1 [cited 2024 Oct 25];9(6). Available from: https://pmc.ncbi.nlm.nih.gov/articles/PMC6597758/

24. Piel L, K. Shanmugha Rajan, Bussotti G, Varet H, Legendre R, Proux C, et al. Experimental evolution links post-transcriptional regulation to Leishmania fitness gain. PLOS Pathogens [Internet]. 2022 Mar 16 [cited 2023 Dec 12];18(3):e1010375–5. Available from: https://journals.plos.org/plospathogens/article?id=10.1371/journal.ppat.1010375

25. LeBowitz JH, Smith HQ, Rusche L, Beverley SM. Coupling of poly(A) site selection and trans-splicing in Leishmania. Genes & Development [Internet]. 1993 Jun 1 [cited 2024 Aug 21];7(6):996–1007. Available from: https://genesdev.cshlp.org/content/7/6/996.long

26. Clayton C. Gene expression in Kinetoplastids. Current Opinion in Microbiology [Internet]. 2016 Aug [cited 2024 Oct 15];32:46–51. Available from: https://www.sciencedirect.com/science/article/pii/S1369527416300534

27. Shapira M, Zilka A, Srinivas Garlapati, Dahan E, Dahan I, Yavesky V. Post transcriptional control of gene expression in Leishmania. Medical Microbiology and Immunology [Internet]. 2001 Sep 7 [cited 2024 Dec 27];190(1-2):23–6. Available from: https://link.springer.com/article/10.1007/s004300100073

28. Cloutier S, Laverdière M, Chou MN, Boilard N, Chow C, Papadopoulou B. Translational Control through eIF2alpha Phosphorylation during the Leishmania Differentiation Process. Moreno SN, editor. PLoS ONE [Internet]. 2012 May 31 [cited 2024 Oct 24];7(5):e35085. Available from: https://pmc.ncbi.nlm.nih.gov/articles/PMC3365078/

29. Genuth NR, Barna M. Heterogeneity and specialized functions of translation machinery: from genes to organisms. Nature Reviews Genetics [Internet]. 2018 May 3 [cited 2024 Dec 27];19(7):431–52. Available from: https://pmc.ncbi.nlm.nih.gov/articles/PMC6813789/

30. McGee JP, Jean-Paul Armache, Lindner SE. Ribosome heterogeneity and specialization of Plasmodium parasites. PLoS Pathogens [Internet]. 2023 Apr 13 [cited 2024 Dec 27];19(4):e1011267–7. Available from: https://pmc.ncbi.nlm.nih.gov/articles/PMC10101515/

31. Norris K, Hopes T, Aspden JL. Ribosome heterogeneity and specialization in development. Wiley Interdisciplinary Reviews - RNA [Internet]. 2021 Feb 9 [cited 2024 Dec 27];12(4). Available from: https://wires.onlinelibrary.wiley.com/doi/10.1002/wrna.1644

32. Shi Z, Fujii K, Kovary KM, Genuth NR, Röst HL, Teruel MN, et al. Heterogeneous Ribosomes Preferentially Translate Distinct Subpools of mRNAs Genome-wide. Molecular Cell [Internet]. 2017 Jul [cited 2024 Oct 25];67(1):71-83.e7. Available from: https://pmc.ncbi.nlm.nih.gov/articles/PMC5548184/

33. Ghulam MM, Catala M, Sherif Abou Elela. Differential expression of duplicated ribosomal protein genes modifies ribosome composition in response to stress. Nucleic Acids Research [Internet]. 2019 Dec 9 [cited 2024 Oct 25];48(4):1954–68. Available from: https://pmc.ncbi.nlm.nih.gov/articles/PMC7038994/

34. Sauert, M., Hannes Temmel and Moll, I. (2014). Heterogeneity of the translational machinery: Variations on a common theme. *Biochimie*, [online] 114, pp.39–47. Doi:https://doi.org/10.1016/j.biochi.2014.12.011.

35. Prossliner T, Winther KS, Sørensen MA, Gerdes K. Ribosome Hibernation. Annual Review of Genetics [Internet]. 2018 Nov 23 [cited 2024 Oct 25];52(1):321–48. Available from: https://pubmed.ncbi.nlm.nih.gov/30476446/

36. Li Y, Sharma MR, Koripella RK, Banavali NK, Agrawal RK, Ojha AK. Ribosome hibernation: a new molecular framework for targeting nonreplicating persisters of mycobacteria. Microbiology [Internet]. 2021 Feb 1 [cited 2024 Oct 25];167(2). Available from: https://pmc.ncbi.nlm.nih.gov/articles/PMC8131030/

37. Ben-Shem A, Jenner L, Gulnara Yusupova, Yusupov M. Crystal Structure of the Eukaryotic Ribosome. Science [Internet]. 2010 Nov 25 [cited 2024 Dec 27];330(6008):1203–9. Available from: https://www.science.org/doi/10.1126/science.1194294

38. Hashem Y, Georges AD, Fu J, Buss SN, Fabrice Jossinet, Jobe A, et al. High-resolution cryo-electron microscopy structure of the Trypanosoma brucei ribosome. Nature [Internet]. 2013 Feb 1 [cited 2024 Dec 27];494(7437):385–9. Available from: https://www.nature.com/articles/nature11872

39. Zhang X, Lai M, Chang W, Yu I, Ding K, Mrázek J, et al. Structures and stabilization of kinetoplastid-specific split rRNAs revealed by comparing leishmanial and human ribosomes. Nature Communications [Internet]. 2016 Oct 18 [cited 2023 Dec 28];7(1). Available from: https://www.nature.com/articles/ncomms13223

40. Oliveros JC. Venny. An interactive tool for comparing lists with Venn's diagrams. https://bioinfogp.cnb.csic.es/tools/venny/index.html [Internet]. Venny. 2007. Available from: bioinfogp.cnb.csic.es/tools/venny/index.html

41. Aslett M, Aurrecoechea C, Berriman M, Brestelli J, Brunk BP, Carrington M, et al. TriTrypDB: a functional genomic resource for the Trypanosomatidae. Nucleic Acids Research [Internet]. 2009 Oct 20 [cited 2024 Dec 27];38(suppl_1):D457–62. Available from: https://pubmed.ncbi.nlm.nih.gov/19843604/

42. Supek F, Matko Bošnjak, Nives Škunca, Tomislav Šmuc. REVIGO Summarizes and Visualizes Long Lists of Gene Ontology Terms. PLoS ONE [Internet]. 2011 Jul 18 [cited 2024 Dec 27];6(7):e21800–0. Available from: https://pmc.ncbi.nlm.nih.gov/articles/PMC3138752/

43. de Pablos LM, Tiago Luiz Ferreira, Dowle A, Forrester S, Parry E, Newling K, et al. The mRNA-bound Proteome of Leishmania mexicana: Novel Genetic Insight into an Ancient Parasite. Molecular & Cellular Proteomics [Internet]. 2019 Jul 1 [cited 2023 Dec 10];18(7):1271–84. Available from: https://www.ncbi.nlm.nih.gov/pmc/articles/PMC6601212/

44. Suradej Siripattanapipong, Parima Boontanom, Saovanee Leelayoova, Mathirut Mungthin, Peerapan Tan-ariya. In vitro growth characteristics and morphological differentiation of Leishmania martiniquensis promastigotes in different culture media. Acta Tropica [Internet]. 2019 May 24 [cited 2024 Nov 4];197:105039–9. Available from: https://www.sciencedirect.com/science/article/pii/S0001706X19305662

45. Juri Ayub M, Levin MJ, Aguilar CF. Overexpression and Refolding of the Hydrophobic Ribosomal P0 Protein from Trypanosoma cruzi: A Component of the P1/P2/P0 Complex. Protein Expression and Purification. 2001 Jul;22(2):225–33.

46. Skeiky YA, Benson DR, Parsons M, Elkon KB, Reed SG. Cloning and expression of Trypanosoma cruzi ribosomal protein P0 and epitope analysis of anti-P0 autoantibodies in Chagas' disease patients. The Journal of Experimental Medicine [Internet]. 1992 Jul 1 [cited 2024 Nov 19];176(1):201–11. Available from: https://pmc.ncbi.nlm.nih.gov/articles/PMC2119278/

47. Arturo J, Carlos Fernando Aguilar. Chagas disease: a homology model for the three-dimensional structure of the Trypanosoma cruzi ribosomal P0 antigenic protein. European Biophysics Journal [Internet]. 2014 Jul 2 [cited 2024 Aug 21];43(8-9):361–6. Available from: https://link.springer.com/article/10.1007/s00249-014-0967-8

48. Kandasamy Saravanakumar, Sathiyaseelan Anbazhagan, Janandi Pujani Usliyanage, Kumar Vishven Naveen, Wijesinghe U, Hu Xiaowen, et al. A comprehensive review on immuno-nanomedicine for breast cancer therapy: Technical challenges and troubleshooting measures. International Immunopharmacology [Internet]. 2021 Dec 16 [cited 2024 Dec 24];103:108433–3. Available from: https://www.sciencedirect.com/science/article/abs/pii/S1567576921010699

49. Brar GA, Weissman JS. Ribosome profiling reveals the what, when, where and how of protein synthesis. Nature Reviews Molecular Cell Biology [Internet]. 2015 Oct 14 [cited 2024 Dec 27];16(11):651–64. Available from: https://pmc.ncbi.nlm.nih.gov/articles/PMC5522010/

50. Beckman Coulter. Instructions For Use SW 41 Ti Swinging-Bucket Rotor [Internet]. 2018 [cited 2024 Dec 26]. Available from: https://bec-techdocs-prod.s3.us-west-2.amazonaws.com/edms/files/L5-TB-047.pdf

51. Vasquez JJ, Hon CC, Vanselow JT, Schlosser A, Siegel TN. Comparative ribosome profiling reveals extensive translational complexity in different *Trypanosoma brucei* life cycle stages. Nucleic Acids Research [Internet]. 2014 Jan 17 [cited 2024 Dec 27];42(6):3623–37. Available from: https://academic.oup.com/nar/article/42/6/3623/2438133

52. Bifeld E, Lorenzen S, Bartsch K, Vasquez JJ, Siegel TN, Clos J. Ribosome Profiling Reveals HSP90 Inhibitor Effects on Stage-Specific Protein Synthesis in *Leishmania donovani*. mSystems [Internet]. 2018 Oct 30 [cited 2024 Nov 5];3(6). Available from: https://journals.asm.org/doi/10.1128/msystems.00214-18

53. Gerashchenko MV, Gladyshev VN. Ribonuclease selection for ribosome profiling. Nucleic Acids Research [Internet]. 2016 Sep 15 [cited 2024 Aug 22];45(2):e6–6. Available from: https://www.ncbi.nlm.nih.gov/pmc/articles/PMC5314788/

54. Shen L, Su Z, Yang K, Wu C, Becker T, Bell-Pedersen D, et al. Structure of the translating *Neurospora* ribosome arrested by cycloheximide. Proceedings of the National Academy of Sciences [Internet]. 2021 Nov 23 [cited 2024 Oct 27];118(48). Available from: https://www.pnas.org/doi/abs/10.1073/pnas.2111862118

55. Mehta P, Woo P, Venkataraman K, Karzai AW. Ribosome Purification Approaches for Studying Interactions of Regulatory Proteins and RNAs with the Ribosome. Methods in molecular biology [Internet]. 2012 Jan 1 [cited 2024 Nov 12];273–89. Available from: https://pmc.ncbi.nlm.nih.gov/articles/PMC4607317/

56. Simsek D, Tiu GC, Flynn RA, Byeon GW, Leppek K, Xu AF, et al. The Mammalian Ribo-interactome Reveals Ribosome Functional Diversity and Heterogeneity. Cell [Internet]. 2017 Jun [cited 2024 Nov 12];169(6):1051-1065.e18. Available from: https://pmc.ncbi.nlm.nih.gov/articles/PMC5548193/

57. Mohammed H, Taylor C, Brown GD, Papachristou EK, Carroll JS, D'Santos CS. Rapid immunoprecipitation mass spectrometry of endogenous proteins (RIME) for analysis of chromatin complexes. Nature Protocols [Internet]. 2016 Jan 21 [cited 2024 Dec 25];11(2):316–26. Available from: https://www.nature.com/articles/nprot.2016.020

58. Vonlaufen N, Kanzok SM, Wek RC, Sullivan WJ. Stress response pathways in protozoan parasites. Cellular Microbiology [Internet]. 2008 Jul 18 [cited 2024 Dec 15];10(12):2387–99. Available from: https://onlinelibrary.wiley.com/doi/10.1111/j.1462-5822.2008.01210.x

59. Balázs Szöör. Trypanosomatid protein phosphatases. Molecular and Biochemical Parasitology [Internet]. 2010 Jun 2 [cited 2024 Dec 15];173(2):53–63. Available from: https://pmc.ncbi.nlm.nih.gov/articles/PMC2994645/

60. Rosenzweig D, Smith D, Myler PJ, Olafson RW, Zilberstein D. Post‐translational modification of cellular proteins during ***Leishmania donovani*** differentiation. PROTEOMICS [Internet]. 2008 Apr 8 [cited 2024 Dec 27];8(9):1843–50. Available from: https://analyticalsciencejournals.onlinelibrary.wiley.com/doi/10.1002/pmic.200701043

61. Hershey JWB. Overview: Phosphorylation and Translation Control. Enzyme [Internet]. 1990 Jan 1 [cited 2024 Dec 7];44(1-4):17–27. Available from: https://pubmed.ncbi.nlm.nih.gov/2133649/

62. Polina Tsigankov, Gherardini PF, Helmer-Citterich M, Späth GF, Myler PJ, Zilberstein D. Regulation Dynamics of Leishmania Differentiation: Deconvoluting Signals and Identifying Phosphorylation Trends. Molecular & Cellular Proteomics [Internet]. 2014 Apr 17 [cited 2024 Dec 7];13(7):1787–99. Available from: https://www.mcponline.org/article/S1535-9476(20)34344-9/

63. Proud CG. Protein Phosphorylation in Translational Control. Current topics in cellular regulation [Internet]. 1992 Jan 1 [cited 2024 Dec 7];243–369. Available from: https://pubmed.ncbi.nlm.nih.gov/1318183/

64. Saxena A, Lahav T, Holland N, Aggarwal G, Anupama A, Huang Y, et al. Analysis of the Leishmania donovani transcriptome reveals an ordered progression of transient and permanent changes in gene expression during differentiation. Molecular and Biochemical Parasitology [Internet]. 2007 Mar [cited 2024 Dec 7];152(1):53–65. Available from: https://pubmed.ncbi.nlm.nih.gov/17204342/

65. Freitas-Mesquita AL, Luiz A, José Roberto Meyer-Fernandes. Involvement of Leishmania Phosphatases in Parasite Biology and Pathogeny. Frontiers in Cellular and Infection Microbiology [Internet]. 2021 Apr 22 [cited 2024 Dec 8];11. Available from: https://pmc.ncbi.nlm.nih.gov/articles/PMC8100340/

66. Deniz Simsek, Barna M. An emerging role for the ribosome as a nexus for post-translational modifications. Current Opinion in Cell Biology [Internet]. 2017 Apr 1 [cited 2024 Dec 27];45:92–101. Available from: https://pubmed.ncbi.nlm.nih.gov/28445788/

67. Filipek K, Blanchet S, Molestak E, Zaciura M, Wu CCC, Patrycja Horbowicz-Drożdżal, et al. Phosphorylation of P-stalk proteins defines the ribosomal state for interaction with auxiliary protein factors. EMBO Reports [Internet]. 2024 Oct 28 [cited 2024 Dec 22];25(12):5478–506. Available from: https://pmc.ncbi.nlm.nih.gov/articles/PMC11624264/

68. Zhou X, Herbst-Robinson KJ, Zhang J. Visualizing Dynamic Activities of Signaling Enzymes Using Genetically Encodable Fret-Based Biosensors. Methods in Enzymology [Internet]. 2012 [cited 2024 Dec 3];317–40. Available from: https://www.sciencedirect.com/science/article/pii/B9780123918574000161

69. Baker N, C. M. C. Catta-Preta, Neish R, J. Sadlova, Powell B, E. V. C. Alves-Ferreira, et al. Systematic functional analysis of Leishmania protein kinases identifies regulators of differentiation or survival. Nature Communications [Internet]. 2021 Feb 23 [cited 2024 Dec 27];12(1). Available from: https://www.nature.com/articles/s41467-021-21360-8

70. Nitika Badjatia, Park SH, Ambrósio DL, Kirkham JK, Günzl A. Cyclin-Dependent Kinase CRK9, Required for Spliced Leader trans Splicing of Pre-mRNA in Trypanosomes, Functions in a Complex with a New L-Type Cyclin and a Kinetoplastid-Specific Protein. PLoS Pathogens [Internet]. 2016 Mar 8 [cited 2024 Dec 2];12(3):e1005498–8. Available from: https://journals.plos.org/plospathogens/article?id=10.1371/journal.ppat.1005498

71. Bhattacharyya A, Kamran M, Ejazi SA, Das S, Didwania N, Bhattacharjee R, et al. Revealing a Novel Antigen Repressor of Differentiation Kinase 2 for Diagnosis of Human Visceral Leishmaniasis in India. Pathogens [Internet]. 2022 Jan 20 [cited 2024 Dec 14];11(2):120. Available from: https://pubmed.ncbi.nlm.nih.gov/35215064/

72. Mathieu Cayla, Y. Romina Nievas, Matthews KR, Mottram JC. Distinguishing functions of trypanosomatid protein kinases. Trends in Parasitology [Internet]. 2022 Sep 5 [cited 2024 Dec 27];38(11):950–61. Available from: https://www.sciencedirect.com/science/article/pii/S1471492222001866

73. Parsons M, Worthey EA, Ward PN, Mottram JC. Comparative analysis of the kinomes of three pathogenic trypanosomatids: Leishmania major, Trypanosoma brucei and Trypanosoma cruzi. BMC Genomics [Internet]. 2005 Sep 15 [cited 2024 Dec 27];6(1). Available from: https://pmc.ncbi.nlm.nih.gov/articles/PMC1266030/

74. Efstathiou A, Smirlis D. Leishmania Protein Kinases: Important Regulators of the Parasite Life Cycle and Molecular Targets for Treating Leishmaniasis. Microorganisms [Internet]. 2021 Mar 27 [cited 2024 Dec 27];9(4):691–1. Available from: https://www.mdpi.com/2076-2607/9/4/691

75. Athina Paterou, Pegine Walrad, Craddy P, Fenn K, Matthews K. Identification and Stage-specific Association with the Translational Apparatus of TbZFP3, a CCCH Protein That Promotes Trypanosome Life-cycle Development. Journal of Biological Chemistry [Internet]. 2006 Oct 17 [cited 2024 Dec 27];281(51):39002–13. Available from: https://pmc.ncbi.nlm.nih.gov/articles/PMC2688685/

76. Héloïse Chassé, Sandrine Boulben, Vlad Costache, Cormier P, Morales J. Analysis of translation using polysome profiling. Nucleic Acids Research [Internet]. 2016 Sep 30 [cited 2024 Dec 27];gkw907–7. Available from: https://academic.oup.com/nar/article/45/3/e15/2972201

77. Sobhany M, Stanley RE. Polysome Profiling without Gradient Makers or Fractionation Systems. Journal of Visualized Experiments [Internet]. 2021 Jun 1 [cited 2024 Dec 20];(172). Available from: https://pmc.ncbi.nlm.nih.gov/articles/PMC8296745/

78. RNasin® Ribonuclease Inhibitor [Internet]. Promega.co.uk. 2024 [cited 2024 Dec 13]. Available from: https://www.promega.co.uk/products/rna-analysis/rnase-inhibitor-rna-protection/rnasin-ribonuclease-inhibitor/?tabset0=0

79. Yamasaki S, Anderson P. Reprogramming mRNA translation during stress. Current Opinion in Cell Biology [Internet]. 2008 Mar 21 [cited 2024 Dec 27];20(2):222–6. Available from: https://www.sciencedirect.com/science/article/abs/pii/S0955067408000306

80. Burki F, Roger AJ, Brown MW, Simpson AGB. The New Tree of Eukaryotes. Trends in Ecology & Evolution [Internet]. 2019 Oct 9 [cited 2024 Dec 27];35(1):43–55. Available from: https://www.cell.com/trends/ecology-evolution/fulltext/S0169-5347(19)30257-5

81. Kohl M, Wiese S, Warscheid B. Cytoscape: Software for Visualization and Analysis of Biological Networks. Methods in Molecular Biology [Internet]. 2010 Oct 13 [cited 2024 Dec 29];291–303. Available from: https://pubmed.ncbi.nlm.nih.gov/21063955/

82. S. Maere, Heymans K, Kuiper M. BiNGO: a Cytoscape plugin to assess overrepresentation of Gene Ontology categories in Biological Networks. Bioinformatics [Internet]. 2005 Jun 21 [cited 2024 Dec 29];21(16):3448–9. Available from: https://pubmed.ncbi.nlm.nih.gov/15972284/

83. Moran Shalev-Benami, Zhang Y, Matzov D, Halfon Y, Zackay A, Rozenberg H, et al. 2.8-Å Cryo-EM Structure of the Large Ribosomal Subunit from the Eukaryotic Parasite Leishmania. Cell Reports [Internet]. 2016 Jul 1 [cited 2024 Dec 29];16(2):288–94. Available from: https://pmc.ncbi.nlm.nih.gov/articles/PMC5835689/

84. Hashem Y, Georges AD, Fu J, Buss SN, Fabrice Jossinet, Jobe A, et al. High-resolution cryo-electron microscopy structure of the Trypanosoma brucei ribosome. Nature [Internet]. 2013 Feb 1 [cited 2024 Dec 29];494(7437):385–9. Available from: https://www.nature.com/articles/nature11872

85. Norris-Mullins B, Krivda JS, Smith KL, Ferrell MJ, Morales MA. Leishmania phosphatase PP5 is a regulator of HSP83 phosphorylation and essential for parasite pathogenicity. Parasitology Research [Internet]. 2018 Jul 7 [cited 2024 Dec 30];117(9):2971–85. Available from: https://link.springer.com/article/10.1007/s00436-018-5994-4#Sec29

86. de la Fuente van Bentem S et al (2005) Heat shock protein 90 and its co-chaperone protein phosphatase 5 interact with distinct regions of the tomato I-2 disease resistance protein. Plant J 43(2):284–298. https://doi.org/10.1111/j.1365-313X.2005.02450.x

87. Nascimento M, Zhang WW, Ghosh A, Houston DR, Berghuis AM, Olivier M, Matlashewski G (2006) Identification and characterization of a protein-tyrosine phosphatase in Leishmania: Involvement in virulence. J Biol Chem 281(47):36257–36268. https://doi.org/10.1074/jbc.M606256200

88. Gómez-Sandoval JN, Escalona-Montaño AR, Abril Navarrete-Mena, M. Magdalena Aguirre-García. Parasite protein phosphatases: biological function, virulence, and host immune evasion. Parasitology Research [Internet]. 2021 Jul 26 [cited 2024 Dec 30];120(8):2703–15. Available from: https://link.springer.com/article/10.1007/s00436-021-07259-9

89. Solari CA, Ortolá Martínez MC, Fernandez JM, Bates C, Cueto G, Valacco MP, et al. Riboproteome remodeling during quiescence exit in Saccharomyces cerevisiae. iScience [Internet]. 2024 Jan [cited 2024 Dec 30];27(1):108727. Available from: https://www.sciencedirect.com/science/article/pii/S2589004223028043

90. Ingolia NT, Ghaemmaghami S, Newman JRS, Weissman JS. Genome-Wide Analysis in Vivo of Translation with Nucleotide Resolution Using Ribosome Profiling. Science [Internet]. 2009 Apr 10 [cited 2024 Nov 5];324(5924):218–23. Available from: https://www.science.org/doi/full/10.1126/science.1168978

91. timsTOF [Internet]. Bruker.com. 2025 [cited 2025 May 4]. Available from: https://www.bruker.com/en/products-and-solutions/mass-spectrometry/timstof.html

92. Skeiky YA, Benson DR, Elwasila M, Badaro R, Burns JM, Reed SG. Antigens shared by Leishmania species and Trypanosoma cruzi: immunological comparison of the acidic ribosomal P0 proteins. Infection and Immunity [Internet]. 1994 May [cited 2025 May 4];62(5):1643–51. Available from: https://pmc.ncbi.nlm.nih.gov/articles/PMC186375/

93. Peacock CS, Seeger K, Harris D, Murphy L, Ruiz JC, Quail MA, et al. Comparative genomic analysis of three Leishmania species that cause diverse human disease. Nature Genetics [Internet]. 2007 Jun 17 [cited 2025 May 4];39(7):839–47. Available from: https://pmc.ncbi.nlm.nih.gov/articles/PMC2592530/

95. Hershey B, Sonenberg N, Mathews MB. Principles of Translational Control: An Overview. Cold Spring Harbor Perspectives in Biology [Internet]. 2012 Dec 1 [cited 2025 May 4];4(12):a011528–8. Available from: https://pmc.ncbi.nlm.nih.gov/articles/PMC3504442/

96. Stryer, L. (1988) Biochemistry. 3rd Edition, W.H. Freeman, San Francisco.

97. Alberts, B. (2015) Molecular Biology of the Cell. 6th Edition, Garland Science, Taylor and Francis Group, New York.

98. Dever TE, Green R. The Elongation, Termination, and Recycling Phases of Translation in Eukaryotes. Cold Spring Harbor Perspectives in Biology [Internet]. 2012 Jul 1;4(7):a013706–6. Available from: https://pmc.ncbi.nlm.nih.gov/articles/PMC3385960/

99. Dinman J, Berry M 2007. Regulation of Termination and Recoding. In Translational control in biology and medicine (ed. Mathews MB, Sonenberg N, Hershey JWB), pp. 625–654 Cold Spring Harbor Laboratory Press, Cold Spring Harbor, NY

100. Lorsch JR, Dever TE. Molecular View of 43 S Complex Formation and Start Site Selection in Eukaryotic Translation Initiation. Journal of Biological Chemistry [Internet]. 2010 Jul; 285(28):21203–7. Available from: https://pubmed.ncbi.nlm.nih.gov/20444698/

101. Janeway CA, Travers P, Walport M, Shlomchik MJ. The structure of a typical antibody molecule [Internet]. Nih.gov. Garland Science; 2025 [cited 2025 May 18]. Available from: https://www.ncbi.nlm.nih.gov/books/NBK27144/

102. RRB1 ribosome biosynthesis protein RRB1 [Saccharomyces cerevisiae S288C] - Gene - NCBI [Internet]. Nih.gov. 2025 [cited 2025 May 18]. Available from: https://www.ncbi.nlm.nih.gov/gene/855161